

UNCLASSIFIED

SECURITY CLASSIFICATION OF THIS PAGE (When Data Entered)

REPORT DOCUMENTATION PAGE		READ INSTRUCTIONS BEFORE COMPLETING FORM
1. REPORT NUMBER Report SIT-DL-78-2020	2. GOVT ACCESSION NO.	3. RECIPIENT'S CATALOG NUMBER
4. TITLE (and Subtitle) AN EXPERIMENTAL STUDY OF A METHOD TO ATTENUATE SURFACE WAVES OVER A LIMITED REGION OF THE OPEN OCEAN		5. TYPE OF REPORT & PERIOD COVERED Final
		6. PERFORMING ORG. REPORT NUMBER SIT-DL-78-2020
7. AUTHOR(s) Richard I. Hires		8. CONTRACT OR GRANT NUMBER(s) N 00014-77-C-0702
9. PERFORMING ORGANIZATION NAME AND ADDRESS DAVIDSON LABORATORY Stevens Institute of Technology Hoboken, New Jersey 07030		10. PROGRAM ELEMENT, PROJECT, TASK AREA & WORK UNIT NUMBERS
11. CONTROLLING OFFICE NAME AND ADDRESS Department of the Navy OFFICE OF NAVAL RESEARCH Arlington, Virginia 22217		12. REPORT DATE June 1978
		13. NUMBER OF PAGES 28 pages; 23 figures
14. MONITORING AGENCY NAME & ADDRESS (if different from Controlling Office)		15. SECURITY CLASS. (of this report) Unclassified
		15a. DECLASSIFICATION/DOWNGRADING SCHEDULE
16. DISTRIBUTION STATEMENT (of this Report) APPROVED FOR PUBLIC RELEASE: DISTRIBUTION UNLIMITED		
17. DISTRIBUTION STATEMENT (of the abstract entered in Block 20, if different from Report)		
18. SUPPLEMENTARY NOTES		
19. KEY WORDS (Continue on reverse side if necessary and identify by block number) Wave Attenuation; Wave-Current Interaction; Wave Refraction		
20. ABSTRACT (Continue on reverse side if necessary and identify by block number) An experimental investigation of the refraction of surface gravity waves by relatively narrow (of the order of or less than one wave length) and shallow, laterally sheared, surface currents was undertaken to determine the feasibility of employing artificially-generated currents to achieve local wave damping in the ocean. In the experiments, single frequency wave trains (wave length, λ_0 , in still water) were initially propagated in the same direction as the direction of the current in the		

wake of a towed grid (with lateral extent, W_g , and draft, d_g). The grid tow speed, U_g , was a small fraction of the wave celerity, c_o . The attenuation, γ_g , of the following waves as they overtook the grid wake and were refracted away from the wake region was determined from wave probes towed along with the grid. The dependence of γ on the dimensionless parameters W_g/λ_o , d_g/λ_o and U_g/c_o was determined and a semiempirical relationship $\gamma = \gamma(W_g/\lambda_o, d_g/\lambda_o, U_g/c_o)$ was developed which provided for a satisfactory collapse of all of the experimental data.

An analysis of the power required to generate an effective current in achieving a specified level of attenuation of an initial wave train was made. The optimal values of the parameters, W_g/λ_o , d_g/λ_o and U_g/c_o which would provide a specified attenuation with minimum expenditure of power were determined. For attenuations from 50 to 70% the required values for these parameters were found to be $W_g/\lambda_o = 0.85$, $0.1 \leq U_g/c_o \leq 0.3$ and $0.14 \leq d_g/\lambda_o \leq 0.17$. The required power for wave lengths up to 300 feet was within the range of installed power of conventional off-shore boats.

STEVENS INSTITUTE OF TECHNOLOGY

**DAVIDSON LABORATORY
CASTLE POINT STATION
HOBOKEN, NEW JERSEY**

Report SIT-DL-78-2020

June 1978

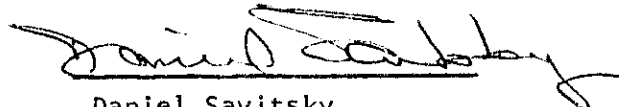
**AN EXPERIMENTAL STUDY OF A METHOD
TO ATTENUATE SURFACE WAVES
OVER A LIMITED REGION OF THE OPEN OCEAN**

by

Richard I. Hires

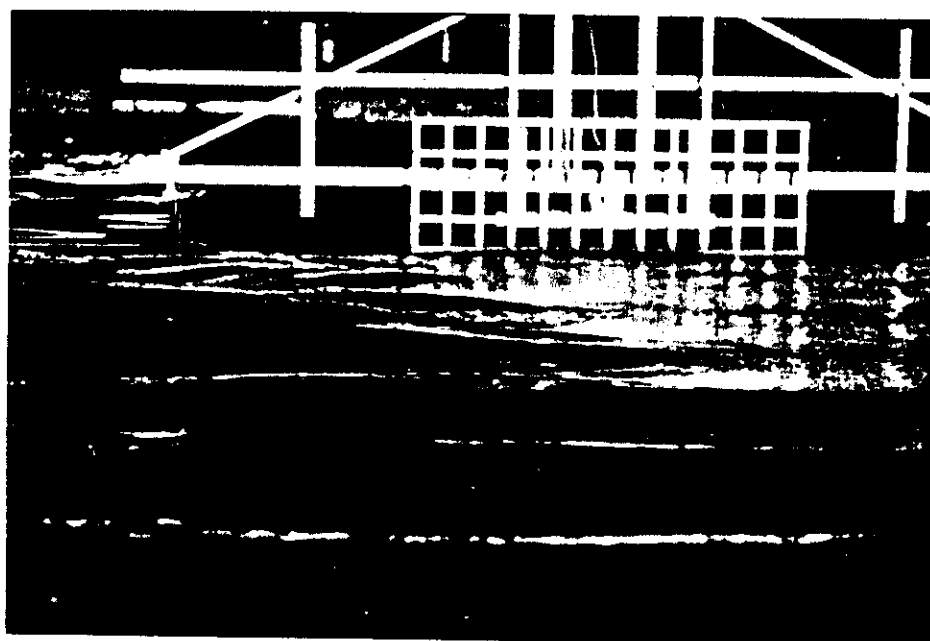
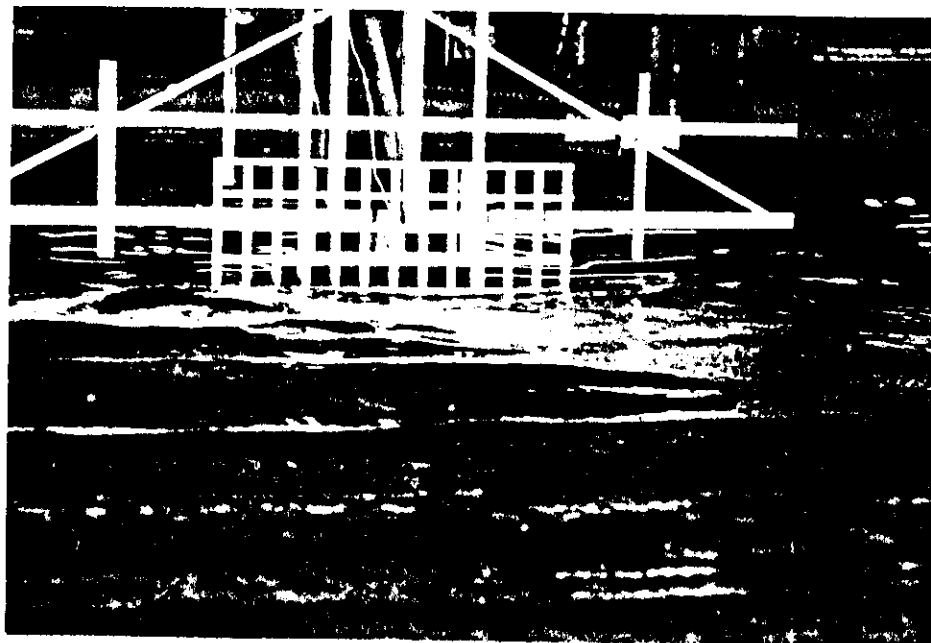
Prepared for
The United States Geological Survey
under
Office of Naval Research Contract
N00014-77-C-0702
(DL Project 4549/034)

Approved:



Daniel Savitsky
Deputy Director

28 pages
23 figures



Photographs of the attenuation of regular waves in the wake of a towed grid. In these photographs the grids are being towed away from the camera. The initial direction of the waves is in the same direction as the direction of tow.

ABSTRACT

An experimental investigation of the refraction of surface gravity waves by relatively narrow (of the order of or less than one wave length) and shallow, laterally sheared, surface currents was undertaken to determine the feasibility of employing artificially-generated currents to achieve local wave damping in the ocean. In the experiments, single frequency wave trains (wave length, λ_o , in still water) were initially propagated in the same direction as the direction of the current in the wake of a towed grid (with lateral extent, W_g , and draft, d_g). The grid tow speed, U_g , was a small fraction of the wave celerity, C_o . The attenuation, γ , of the following waves as they overtook the grid wake and were refracted away from the wake region was determined from wave probes towed along with the grid. The dependence of γ on the dimensionless parameters W_g/λ_o , d_g/λ_o and U_g/C_o was determined and a semiempirical relationship $\gamma = \gamma(W_g/\lambda_o, d_g/\lambda_o, U_g/C_o)$ was developed which provided for a satisfactory collapse of all of the experimental data.

An analysis of the power required to generate an effective current in achieving a specified level of attenuation of an initial wave train was made. The optimal values of the parameters, W_g/λ_o , d_g/λ_o and U_g/C_o which would provide a specified attenuation with minimum expenditure of power were determined. For attenuations from 50 to 70% the required values for these parameters were found to be $W_g/\lambda_o = 0.85$, $0.1 \leq U_g/C_o \leq 0.3$ and $0.14 \leq d_g/\lambda_o \leq 0.17$. The required power for wave lengths up to 300 feet was within the range of installed power of conventional off-shore boats.

KEYWORDS

Wave Attenuation

Wave-Current Interaction

Wave Refraction

TABLE OF CONTENTS

ABSTRACT.....	i
I. INTRODUCTION.....	1
II. DESCRIPTION OF EXPERIMENTS.....	5
III. EXPERIMENTAL RESULTS.....	6
IV. ANALYSIS OF EXPERIMENTAL RESULTS.....	10
V. MINIMUM POWER REQUIREMENTS.....	21
VI. SUMMARY AND DISCUSSION OF RESULTS.....	25
VII. REFERENCES.....	28
FIGURES (1-23)	

1. INTRODUCTION

Wind-generated surface waves comprise a critical environmental constraint on the conduct of a wide variety of operations at sea. The likelihood of failure to accomplish the objectives of an operation and the risks to personnel clearly rise as increasingly higher sea states are encountered. Conversely, if the surface waves could be significantly attenuated for even relatively short durations and over a limited region of the ocean, then the likelihood of the successful and safe completion of an operation could be markedly enhanced. The overall purpose of the present experimental study was to investigate the feasibility of achieving significant local attenuation of waves through refraction effects produced by an artificially generated surface current. The underlying principle in this approach is that the wave celerity will be altered by the interaction of the waves with the artificially produced current and that the subsequent refraction of the waves can lead to substantial local attenuation of the waves.

A phenomenological explanation for the effect of an artificially generated current on refraction and subsequent attenuation of waves can be obtained from a consideration of the following simplified case. A wave train is assumed to propagate in the positive x -direction in the undisturbed ocean. At $x = 0$, the waves encounter a current also flowing in the positive x -direction. The current is of finite width and exhibits symmetric lateral shear about its axis, $y = 0$, where the current speed, U , is a maximum. Figure 1 is a sketch of the physical situation described above. Prior to encountering the current, i.e., for $x < 0$, the crest lines for the wave train are straight lines parallel to the y -axis while the orthogonal wave rays are parallel to the x -axis. Upon encountering the current, the portion of the waves within the current increase in speed relative to that outside of the current. The crestlines subsequently are deformed in the manner shown in Figure 1. The wave rays which indicate the direction of propagation of the deformed wave train diverge

about the axis of the current. The wave train consequently is refracted away from the axis of the current and in this region the waves will be attenuated.

This attenuation can be explained by consideration of the power transmitted by the refracted waves. The basis of this explanation is the assumption that the transmitted power between adjacent wave rays remains constant. The wave power per unit length along the crestline, P_w , is the product of the local wave energy per unit area E_w and the speed of energy propagation, V , i.e.,

$$P_w = E_w V \quad (1)$$

and for deep water gravity waves

$$P_w = 1/8 \rho g H^2 (C_g + U \cos \alpha) \quad (2)$$

where:

ρ = water density,

g = acceleration of gravity,

H = wave height,

C_g = local group velocity of the waves relative to the water,

$U \cos \alpha$ = velocity component aligned with the direction of wave propagation.

In still water, $x < 0$, the power transmitted between adjacent wave rays separated by a distance ℓ_o would be

$$P_{wo} \ell_o = 1/8 \rho g H_o^2 C_{go} \quad (3)$$

while within the current where the separation is ℓ then

$$P_w \ell = 1/8 \rho g H^2 (C_g + U \cos \alpha) \quad (4)$$

Since $P_w \ell = P_{w0} \ell_0$ then

$$\frac{H}{H_0} = \left(\frac{\ell_0}{\ell} \right)^{\frac{1}{2}} \left(\frac{C_{g0}}{C_g + U \cos \alpha} \right)^{\frac{1}{2}} \quad (5)$$

With divergent wave rays ℓ_0/ℓ must be less than unity and with an assisting current, the ratio $(C_g/(C_g + U \cos \alpha))$ will also be less than one and consequently wave heights will be attenuated within the current, i.e., $H/H_0 < 1$.

Savitsky¹ conducted a limited series of experiments which demonstrated the attenuation of waves in the laterally sheared wake of a grid towed in the same direction as that of the initial wave train. In Savitsky's experiments long crested waves propagated into a relatively narrow and shallow wake produced by a three-foot wide grid towed in a 75-foot square tank. The width of the grid-generated wake was of the same order as the wavelengths employed in the experiments while the draft of the grid was as small as 14% of the longest wavelength and the tow speed was as small as 20% of the wave celerity. The attenuation of wave heights in the wake of the grid was dramatic with values ranging up to 90%. The results obtained by Savitsky suggest that it would be possible to attain similar local attenuation of waves in the ocean by perhaps employing tugs to tow a suitably larger version of Savitsky's grid. It should be noted here that the original intent of Savitsky's work was to make a fundamental study of the interaction of the waves with the turbulence in the wake which, unfortunately, was found to be all but completely masked by the extreme deformation of the waves achieved through the refraction of the wave train by the mean velocity distribution. As a consequence of this underlying purpose of Savitsky's work, his experimental program was not sharply focused on a fundamental study of wave refraction by currents nor on how this procedure could be adapted for practical use in the ocean.

The present experimental study was a continuation of the work initiated by Savitsky. One objective of the experimental program was to determine the empirical functional relationship between wave attenuation and the characteristics of both the laterally sheared current and the initial wave train. A second objective was to determine the minimum power required to generate a flow field sufficient to achieve a prescribed degree of wave attenuation under a given set of initial wave conditions. In the present experiments, grids similar to those employed by Savitsky, were used to generate the sheared surface currents. The power required to tow the grids at a speed U_g through the water is

$$P_G = \frac{1}{2} \rho C_D U_g^3 W_g d_g$$

where:

C_D = drag coefficient

W_g = the width of the grid

d_g = the grid draft

The required power can be expressed alternatively in terms of non-dimensional parameters relating the grid characteristics to the wave length, λ_o , and celerity, C_o , of the initial wave train, i.e.,

$$P_G = \frac{1}{2} \rho C_o \left(\frac{U_g}{C_o}\right)^3 \left(\frac{W_g}{\lambda_o}\right) \left(\frac{d_g}{\lambda_o}\right) C_o^3 \lambda_o^2$$

The specific objectives of the experimental work were to determine the dependence of the wave attenuation, $\gamma \equiv (H_o - H)/H_o$, on the dimensionless parameters, U_g/C_o , W_g/λ_o , d_g/λ_o , and then to determine the combination of these parameters which will provide the desired attenuation with minimum expenditure of power.

There exists several theoretical studies of various aspects of the interaction and refraction of waves with currents^{2,3,4,5,6} but none are strictly applicable to the above-described conditions. The results of the

available theory do, however, provide a framework for the formulation of the empirical relationship

$$\gamma = \gamma(U_g/C_o, W_g/\lambda_o, d_g/\lambda_o).$$

The application of theoretical results for some oversimplified cases to the analysis of the experimental results will be presented in Chapter IV of this report following a description of the experiments.

II. DESCRIPTION OF EXPERIMENTS

The experimental study was conducted in a 75-foot square, 4½-foot deep towing tank* with a wavemaker along one side of the tank and a beach on the opposite side. The grids, constructed of crossed, ¾" square wooden slates on 4" centers, were attached through a stiff spring drag balance to a carriage mounted on the overhead rail. The carriage in turn is attached to a continuous chain which runs over a cone of sprockets driven by a servo controlled DC motor. The carriage speed is determined from measurement of the travel time between fixed points on the rail. Figure 2a is a schematic sketch of the setup for towing the grids.

Wave heights were measured using an array of impedance-type wave probes which were supported from auxiliary carriages on the overhead rail and were towed with the grid. The arrangement of the wave probes is shown schematically in Figure 2b. Probe No. 1 was fixed on the centerline of the grid wake and its distance aft of the grid could be incrementally varied. Probe No. 2 was fixed to a traversing mechanism which allowed for the determination of the lateral distribution of wave heights in the grid wake during the course of a run. Probes 3 and 4 revealed the wave conditions outside of the wake region and Probe No. 6 measured wave conditions directly in front of the grid. The output signals from the wave probes, together with the outputs from the drag balance and the position indicator on the traversing mechanism were transmitted to shore via overhead cables, amplified and recorded on an oscillograph.

*This is the same facility which Savitsky used for his experiments.

The determination of the velocity distributions in the grid wake were made using a hot-film anemometer. The hot-film probe was traversed laterally and vertically at several distances aft of the grid to establish the velocity distribution. The DISA anemometer and linearizer provided an output signal linearly proportional to current speed. Since the probe was towed through the water at the grid tow speed, U_g , and the water speed in the wake, U_w , was less than U_g , then the current speed measured by the hot-film anemometer, U_a is the difference between the tow speed and the wave velocity and, consequently, $U_w = U_g - U_a$. It should be noted that the hot-film anemometry measurements were made without waves.

In the experiments, 3 grids were employed with widths of 2, 4 and 8 feet. The grid draft could be varied in one inch increments to a maximum immersion depth of 24 inches. The grid tow speed could be varied continuously up to 4 feet/sec, but with wider grids at large drafts the maximum obtainable speed was reduced by the power limitation on the motor for the carriage drive. The range of wave lengths used in the experiments ranged from 2 to 16 feet. The initial wave heights were varied from 1 to 3 inches.

III. EXPERIMENTAL RESULTS

The velocity distributions in the wake of the towed grids obtained from the hot-film anemometer measurements are shown in Figures 3-12. The top panel in each figure presents contours of the ratio of the wake speed to the grid tow speed, U_w/U_g , in the vertical plane at the indicated distance aft of the grid. Since the wake can be assumed to be symmetric about the centerline of the grid, measurements were limited to just one side of the longitudinal axis of the wake and consequently, the distributions in the figures are assumed assymmetric about the centerline. The grid draft and half width are also shown in the upper panel of these figures. The lower half of each of these figures shows the lateral distribution of measured velocities at fixed depths. The bulk of the hot film measurements were obtained with the 2-foot wide grid. Figures 3-10 show

the results for this grid and Figures 11 and 12 the results for a limited series of measurements with the 4-foot wide grid.

Figures 3 and 4 depict the results for a grid draft of 4 inches at distances 6 and 12 feet aft of the 2-foot wide grid, respectively. For this draft the maximum wake velocity at 6 feet aft occurs approximately at the depth of the grid draft, while at 12 feet the maximum currents occur at depths greater than the draft of the grid. The maximum center-line velocity ratio U_w/U_g decreases from 0.45 to 0.19 as the distance aft of the grid is doubled. Figures 5 and 6 reveal similar results for 8-inch grid draft. The maximum velocity ratio is marginally higher with the increased grid draft but the variation with longitudinal distance is strikingly similar to that obtained with the 4-inch draft. Figure 7 shows the distribution 6 feet aft of the grid for 16-inch draft. For this deeper draft the maximum wake velocity occurs at the surface and the distribution exhibits nearly uniform speeds near the surface from the centerline to 6-8 inches off the centerline.

Figures 8, 9 and 10 show the velocity distributions 3, 6 and 12 feet aft of the 2-foot wide grid at its maximum draft of 24 inches. The maximum wake velocity occurs at the surface at each distance aft of the grid with the maximum speed decreasing by about a factor of 2 as the distance aft increases from 3 to 12 feet. At 3 and 6 feet aft of the grid the velocity is relatively uniform over approximately the central two thirds of the lateral extent of the grid.

Finally, Figures 11 and 12 show the velocity distributions at 6 feet aft of the 4-foot wide grid for grid drafts of 4 and 8 inches. These distributions are remarkably similar to those obtained with the 2-foot wide grid at the same drafts shown in Figures 3 and 5.

An example of the results obtained in the experimental runs to determine the wave attenuation in the wake of the grid is presented in Figure 13. The positions of the wave probes relative to the grid are shown in Figure 2b. The initial wave heights before the grid is moved

revealed no significant differences between wave probes behind and in front of the grid, which indicates that the grid was essentially transparent to the waves. Once the grid begins to move, the wave heights measured by probe No. 1 and the traversing wave probe (No. 2) decrease for a relatively short interval of time while the wake becomes established and then reach a steady value. During this same interval the wave heights measured by probes 3 and 4 located outside of the wake increased as would be expected if the wave energy is refracted away from the axis of the grid wake. The variation of the wave heights as probe No. 2 is traversed laterally through the wake shows the effective width of the region in which waves are significantly attenuated and the increase in wave heights to values greater than the undisturbed heights as the probe moves laterally beyond the boundary of the wake.

Clearly the most important measurement to be obtained from the wave records is the ratio of the steady wave heights in the wake, H , as measured by probe No. 1 to the initial wave height, H_0 , from which the attenuation $\gamma \equiv 1 - (H/H_0)$ can be obtained. Figure 14 is an example of the typical variations of the experimentally determined values of γ with the parameters U_g/C_0 (Figure 14a), d_g/λ_0 (Figure 14b) and W_g/λ_0 (Figure 14c). Figure 14a reveals that for small values of U_g/C_0 the attenuation increases with increasing values of this speed ratio while at larger values the attenuation becomes nearly constant. A similar pattern for the attenuation is shown in Figures 14b and 14c for increasing values of d_g/λ_0 and W_g/λ_0 respectively. Two additional and extremely significant features of the experimental results are shown in Figures 14a and 14b. In Figure 14a variations of γ with U_g/C_0 for initial wave heights of 1.5 and 3.0 inches are shown to be virtually identical. In Figure 14b the variation in γ with d_g/λ_0 for $W_g = 2$ feet and $\lambda_0 = 6$ feet is very similar to the variation obtained with $W_g = 4$ feet and $\lambda_0 = 12$ feet.

It should be emphasized that the results summarized in Figure 14 are drawn from only a small fraction of the total number of experimental runs. They are, however, representative and consistent with all of the

remainder of the observations. A detailed analysis of the dependence of the attenuation on U_g/C_o , d_g/λ_o and W_g/λ_o is presented in Chapter IV.

The attenuation of waves with U_g/C_o , d_g/λ_o , and W_g/λ_o held constant was found to decrease as the distance between the grid and wave probe No. 1 was increased. Figure 15 is an example of the variation of attenuation with U_g/C_o at 4 and 14 feet aft of the grid. Since the results of the velocity surveys in the wake revealed a marked decrease in U_w/U_g with increasing distance aft of the grid, it is expected that to obtain the same attenuation at 14 feet as that at 4 feet the ratio of U_g/C_o would have to be substantially increased. The results presented in Figure 15 confirm this expectation and suggest that the attenuation within the wake at a given distance aft of the grid depends on the current speed at that location.

The results of the determination of the width of the attenuated region in the wake by use of the traversing wave probe revealed no clearly defined dependence on either U_g/C_o or d_g/λ_o . The ratios of the width of the attenuated region, b , to the grid width, W_g , exhibited substantial scatter which could be attributed to the difficulty in the accurate determination of b . The averages of all values of b/W_g obtained for constant values of W_g/λ_o did reveal a dependence of b/W_g on W_g/λ_o with the width of the attenuated region increasing with increasing wave lengths for a given grid width. Figure 16 shows this variation of b/W_g with W_g/λ_o .

A series of experiments were performed to determine the duration of the attenuation in the wake following the passage of the grid. A stationary wave probe was mounted in the axis of the wake near the midpoint of the distance traversed by the grid during an experimental run. The grid was modified so that it could pass unimpeded over the wave probe. The duration of attenuation was determined from the time history of the wave record obtained from the stationary probe. The duration of attenuation was defined to be the time interval between the passage of the grid and the occurrence of a noticeable recovery of the wave heights towards

their initial values. An example of the results obtained in this limited series of experiments is shown in Figure 17. In this figure, data is presented for two sets of experiments. Within each set are two series of experiments under geometrically similar conditions, i.e., W_g/λ_o and d_g/λ_o are constant, but the scale of one series is twice that of the other. A reasonable agreement between the geometrically similar series is obtained by assuming that the duration is dependent on the Froude Number and consequently the duration time should vary as the square root of the length scale. In Figure 17 the durations obtained using the smaller grid have been multiplied by $\sqrt{2}$ to illustrate this apparent Froude Number dependence.

The drag measurements were used to obtain values of the drag coefficient, C_D , for the grid where

$$C_D = \frac{\text{Drag}}{\frac{1}{2} \rho U_g^2 W_g d_g} .$$

During each experimental run the drag balance output, linearly proportional to drag, was averaged over the same distance of travel of the grid as that used to determine the carriage speed. The drag coefficient was found to be independent of the grid tow speed and its average value determined from over 500 experimental runs was 0.65.

IV. ANALYSIS OF EXPERIMENTAL RESULTS

Insight into the processes contributing to the attenuation of surface waves in the wake of towed grids can be obtained by consideration of some oversimplified cases. With a co-ordinate system chosen such that the origin is at the undisturbed water surface, the z-axis oppositely directed to the acceleration of gravity, we consider as a first case the interaction of a long crested surface wave train propagating in the positive x direction with a variable current $U = U(x, \text{only})$. This problem has been addressed by Phillips² and his analysis is reproduced here in order to serve as an introduction to the more complex cases.

It will prove useful to develop first the properties of the wave train in still water, i.e., $U = 0$, and then proceed to the case where $U \neq 0$. In still water the wave profile is given by

$$\eta = a_0 \cos(k_0 x - \sigma_0 t)$$

where a_0 = wave amplitude

$$k_0 = 2\pi/\lambda, \lambda_0 = \text{wave length}$$

$$\sigma_0 = 2\pi/T, T_0 = \text{wave period}$$

and the wave is propagating in the positive x -direction with phase speed $C_0 = \sigma_0/k_0$. Since it can be assumed that the wave motion is irrotational, incompressible and inviscid then the velocity potential for the motion, φ , must satisfy Laplace's equation

$$\nabla^2 \varphi = 0$$

The velocity field \vec{V} is related to φ by

$$\vec{V} = u\vec{i} + w\vec{k} = -\nabla\varphi.$$

The exact boundary conditions on φ are as follows: at the free surface, $z = \eta = 0$, the kinematic boundary condition is

$$\left[\frac{D}{Dt} (z - \eta) \right]_{z=\eta} = 0$$

or, since

$$\frac{Dz}{Dt} \equiv w = -\frac{\partial \varphi}{\partial z}$$

then

$$-\frac{\partial \varphi}{\partial z} \bigg|_{z=\eta} = \frac{\partial \eta}{\partial t} + u \frac{\partial \eta}{\partial x} + w \frac{\partial \eta}{\partial z}.$$

The dynamic boundary condition at $z = \eta$ is that $p|_{z=\eta} = p_0$ where p_0 is the assumed constant air pressure. By applying Bernoulli's equation we obtain

$$g\eta - \frac{\partial \varphi}{\partial t} \Big|_{z=\eta} + \frac{1}{2}(u^2 + w^2) \Big|_{z=\eta} = 0$$

where we have neglected surface tension.

Finally, the kinematic condition at the bottom $z = -D$ is

$$\frac{D(z+d)}{Dt} \Big|_{z=-D} = 0$$

or

$$\frac{\partial \varphi}{\partial z} \Big|_{z=-D} = \frac{\partial D}{\partial t} + u \frac{\partial D}{\partial x} + w \frac{\partial D}{\partial z}$$

If we assume $D = \text{constant}$, $U = 0$, and linearize the free surface boundary conditions by expanding φ in powers of the wave slope $a\kappa$ then the set of equations to be solved, correct to first order in $a\kappa$, are:

$$\nabla^2 \varphi = 0$$

$$-\frac{\partial \varphi}{\partial z} \Big|_{z=0} = \frac{\partial \eta}{\partial t}, \quad \frac{\partial \varphi}{\partial z} \Big|_{z=-D} = 0$$

$$\frac{\partial \varphi}{\partial t} \Big|_{z=0} = g\eta$$

The well known solution² is

$$\varphi = -a_o \sigma_o \frac{\cosh \kappa_o(z+D)}{\sinh \kappa_o D} \sin(\kappa_o x - \sigma_o t)$$

and the dynamic boundary condition yields a relationship between σ_o and κ_o , namely

$$\sigma_o^2 = g\kappa_o \tanh \kappa_o D$$

and

$$c_o^2 = \sigma_o^2 / \kappa_o^2 = g / \kappa_o \tanh \kappa_o D$$

For water depths greater than $\lambda/2$ the waves may be considered to be in deep water and in this case

$$\varphi_0 = -a_0 \frac{\sigma_0}{\kappa_0} e^{\kappa_0 z} \sin(\kappa_0 x - \sigma_0 t)$$

$$c_0^2 = g/\kappa_0$$

With a current present, i.e., $U \neq 0$, it is convenient to define φ as pertaining only to the wave motion and let u' , w' be the velocity components of the wave motion. The linearized boundary conditions become for this case:

$$-\left. \frac{\partial \varphi}{\partial z} \right|_{z=0} = \frac{\partial \eta}{\partial t} + U \frac{\partial \eta}{\partial x}, \quad \left. \frac{\partial \varphi}{\partial z} \right|_{z=-D} = 0,$$

$$\left. \frac{\partial \varphi}{\partial t} \right|_{z=0} = g\eta - U \left. \frac{\partial \varphi}{\partial x} \right|_{z=0}$$

For a wave train in deep water the solution for φ is

$$\varphi = -\frac{a(\sigma - \kappa U)}{\kappa} e^{\kappa z} \sin(\kappa x - \sigma t)$$

and the relation between σ and κ is

$$(\sigma - \kappa U) \sigma / \kappa = g + U(\sigma - \kappa U)$$

which reduces to

$$\sigma / \kappa = \sqrt{g/\kappa} + U.$$

The quantity σ/κ is the wave celerity relative to fixed co-ordinates and $C = \sqrt{g/\kappa}$ is the wave celerity relative to the moving water. We can define a frequency, n , for the waves which would be observed in a reference frame translating with the water current. Since $C = n/\kappa = \sqrt{g/\kappa}$ then

$$\sigma / \kappa = n / \kappa + U$$

or

$$n = \sigma - \kappa U$$

Phillips² presents arguments that σ must remain constant as the waves encounter a current and if $\sigma = \sigma_0 = \text{constant}$, then

$$n + \kappa U = \sigma_0 .$$

Since

$$n + \kappa U = \kappa(C + U)$$

$$\sigma_0 = C_0 \kappa_0$$

then

$$C_0 \kappa_0 = \kappa(C + U)$$

and

$$\kappa_0 / \kappa = (C + U) / C_0 .$$

Also, since

$$C = \sqrt{g/\kappa} , \quad C_0 = \sqrt{g/\kappa_0}$$

then

$$C^2 / C_0^2 = \kappa_0 / \kappa = (C + U) / C_0$$

and, finally

$$C / C_0 = \frac{1}{2} + \frac{1}{2} [1 + 4U/C_0]^{\frac{1}{2}} .$$

This last result can be recast as

$$(C + U) / C_0 = \frac{1}{2} + U/C_0 + \frac{1}{2} [1 + 4U/C_0]^{\frac{1}{2}} . \quad (6)$$

Equation (6) is a useful first result in considering the refraction of waves by currents even though it applies in a strict sense only to the two-dimensional wave current interaction problem. We can interpret $(C + U)/C_0$ as the ratio of the wave propagation speed in the current, e.g., along with centerline of the grid wake, to the wave celerity outside of the wake. From a non-rigorous standpoint this ratio is in essence one measure of the refractive capability of the wake's velocity distribution. If other parameters such as the lateral velocity distribution and the width of the wake are held constant then the intensity of refraction and, hence, degree of attenuation, should increase with increasing values of $(C + U)/C_0$.

In the present experiments we have one additional complication which must be considered, namely that the velocity field in the wake has a finite depth, d , which is not large compared to the wavelengths of the waves encountering this wake. Equation (6) was developed on the basis of a deep current which was uniform with depth. We shall now develop the effect of a surface current of finite depth, d , on a wave train with wavelength λ in which λ may be considerably larger than d . This development follows that of Taylor.³ The surface current is assumed to be uniform from the surface to the depth $z = -d$ and is zero below this depth. The wave profile at the surface is $\eta_s = a \cos(\kappa x - \sigma t)$. At $z = -d$, the boundary between the surface current and the quiescent water below is perturbed due to the wave motion. This disturbance is represented by $\eta_\ell = b \cos(\kappa x - \sigma t)$. In the surface layer we can define a velocity potential φ_1 associated with the wave motion while below $z = -d$ the velocity potential is φ_2 .

$$\eta_s \geq z \geq (-d + \eta_\ell) ,$$

$$\nabla^2 \varphi_1 = 0 ,$$

and for

$$z \leq (-d + \eta_\ell) ,$$

$$\nabla^2 \varphi_2 = 0 .$$

The boundary conditions on φ_1 are, correct to first order in $a\kappa$,

$$-\left.\frac{\partial\varphi_1}{\partial z}\right)_{z=0} = \frac{\partial\eta_s}{\partial t} + u \frac{\partial\eta_s}{\partial x}, \quad (7)$$

$$-\left.\frac{\partial\varphi_1}{\partial z}\right)_{z=-d} = \frac{\partial\eta_\ell}{\partial t} + u \frac{\partial\eta_\ell}{\partial x}, \quad (8)$$

and

$$\left.\frac{\partial\varphi_1}{\partial t}\right)_{z=0} = g\eta_s - u \left.\frac{\partial\varphi}{\partial x}\right)_{z=0}. \quad (9)$$

The kinematic boundary conditions on φ_2 are

$$\frac{\partial\varphi_2}{\partial x}, \frac{\partial\varphi_2}{\partial y} \rightarrow 0 \text{ as } z \rightarrow -\infty \quad (10)$$

and

$$-\left.\frac{\partial\varphi_2}{\partial z}\right)_{z=-d} = \frac{\partial\eta_\ell}{\partial t}. \quad (11)$$

The dynamic boundary condition at $z = -d$ is that $p_1 = p_2$ which yields

$$\left.\frac{\partial\varphi_1}{\partial t}\right)_{z=-d} + u \left.\frac{\partial\varphi_1}{\partial x}\right)_{z=-d} = \left.\frac{\partial\varphi_2}{\partial t}\right)_{z=-d}. \quad (12)$$

The solutions for φ_1 and φ_2 are

$$\varphi_1 = (Ae^{\kappa z} + Be^{-\kappa z}) \sin(\kappa x - \sigma t) \quad (13)$$

$$\varphi_2 = (Ce^{\kappa(z+d)} + De^{-\kappa(z+d)}) \sin(\kappa x - \sigma t) \quad (14)$$

From (10) we can set $D = 0$ and we can use equations (7), (8), (9), (10) and (11) to determine the constants A , B , C , b , and the relationship between σ and κ . Substitution of equations (13) and (14) into the boundary conditions yields

$$(-A + B)\kappa = a(\sigma - \kappa U) \quad (15)$$

$$(-Ae^{-\kappa d} + Be^{\kappa d})\kappa = b(\sigma - \kappa U) \quad (16)$$

$$(A+b)(-\sigma + \kappa U) - ga = 0 \quad (17)$$

$$-\kappa C = \sigma b \quad (18)$$

$$(Ae^{-\kappa d} + Be^{\kappa d})(-\sigma + \kappa U) = -\kappa C \quad (19)$$

Since our chief concern is the relationship between σ and κ we can eliminate a , b , A , B and C from Equation (15) through (16) to find

$$\frac{(\sigma - \kappa U)^4 - \kappa g \sigma^2}{(\sigma - \kappa U)^2 (\sigma^2 - g\kappa)} = -\coth \kappa d \quad (20)$$

From our previous discussion we can identify σ as the invariant wave frequency relative to a fixed co-ordinate system and $C_B = \sigma/\kappa$ is the wave celerity over the bottom. The wave celerity in still water is $C_o = g/\sigma$. The ratio of the wave celerity, C_B to C_o is

$$\frac{C_B}{C_o} = \frac{\sigma^2}{\kappa g} \equiv \frac{1}{X}.$$

This ratio has the identical significance to the ratio $(C+U)/C_o$ which was developed for the case of deep currents. The ratio of the surface current speed U to the wave celerity σ/κ is

$$\frac{\kappa U}{\sigma} \equiv Y.$$

Finally, we can identify $U/\sqrt{gd} \equiv F$, as the Froude number based on the depth of the current. With the non-dimensional quantities X , Y and F we can rewrite Equation (20) as

$$-\frac{(1-Y)^4 - X}{(1-Y)^2 (1-X)} = \coth\left(\frac{Y^2}{F^2 X}\right) \quad (21)$$

Since σ , U , g , d can be considered as known in our experiments, then we can find F and the ratio of Y/X . Equation (21) may then be used to determine $1/X$ for any given set of experimental conditions.

Equation (21) can be exploited to reveal the dependence of C_B/C_O on the ratio of the depth of the current to the wavelength in still water, d/λ_O . Plots of C_B/C_O against d/λ_O for several ratios of U/C_O are presented in Figure 18. For d/λ_O greater than about 0.5 the value of C_B/C_O coincides closely with the values $(C+U)/C_O$ calculated for an infinitely deep current. The effect of finite current depth on C_B/C_O is most pronounced for d/λ_O less than 0.1 where C_B/C_O decreases nearly linearly to unity as the ratio of d/λ_O approaches zero.

The ratio of the wave celerity C_B which a wave train would attain along the centerline of the symmetrically sheared wake aft of the towed grids, to the wave celerity, C_O , outside of the wake is again assumed to be a measure of the refractive capacity of the wake. In order to calculate C_B/C_O it is necessary to know the current speed U on the centerline and the effective depth of the current. The hot-film anemometry work suggests that for distances of 3-6 feet aft of the grid $U \sim 0.5 U_g$ where U_g is the grid tow speed. The wake velocity on the centerline is nearly uniform with depth to about the draft of the grid. Below this depth the velocity decreases to zero. As a first approximation we can characterize the current along the centerline as having uniform speed from the surface to a depth $d = d_g$, with this speed equal to $0.5 U_g$. Below the depth of the grid draft the current will be assumed to vanish. With this simplification, the ratio C_B/C_O can be obtained from Equation (21) for each experimental run. The value of C_B/C_O thus obtained will, of course, be strictly applicable for the case of the wave train encountering a current which is uniform in the lateral direction, i.e., Equation (21) was derived on the basis of a two rather than three-dimensional analysis. In the experiments the width of the grid wake was clearly finite and in most instances a relatively small fraction of the wavelength of the incident waves. It should be anticipated that the actual wave celerity

along the centerline of the wake will be dependent upon the ratio W_g/λ_o . For large values of this ratio the value of C_B/C_o would approach that predicted by the two-dimensional theory, while for smaller values of W_g/λ_o the actual celerity along the centerline would depart significantly from the theoretical result.

In order to test the hypothesis that the wave attenuation depends on the computed values of C_B/C_o the experimental results were divided into groups in which W_g/λ_o was constant. For each group the experimentally determined values of the wave attenuation were plotted against the calculated value of C_B/C_o . Since the velocity used to determine C_B/C_o was assumed to be $0.5 U_g$, which approximated the wake centerline velocity at distances less than about 6 feet from the grids, only experimental runs where the attenuation was measured within this distance from the grid were used in the plots of γ against C_B/C_o . Figures 19 and 20 are plots of γ against C_B/C_o for $W_g/\lambda_o = 0.33$ and $W_g/\lambda_o = 1$. These reveal a linear dependence of attenuation on the ratio C_B/C_o until the attenuation reaches values of about 80% at which point the attenuation remains nearly constant with increasing values of C_B/C_o . The plotted points in each of these figures were for experimental runs employing wide ranges of the parameters U_g/C_o and d_g/C_o . The collapse of the experimentally determined attenuation data when plotted against C_B/C_o , which was found for each group of experimental runs within which W_g/λ_o was constant, suggest that an empirical relationship for the attenuation would have the form

$$\gamma = F\left(\frac{W_g}{\lambda_o}\right) \left[\frac{C_B}{C_o} - 1\right] .$$

This relationship would only be appropriate for the range of values C_B/C_o for which γ increases linearly with increasing values of C_B/C_o . The as yet unspecified functional dependence of γ on W_g/λ_o should exhibit the following properties:

$$\lim_{W_g/\lambda_o \rightarrow 0} F(W_g/\lambda_o) \rightarrow 0$$

$$\lim_{W_g/\lambda_o \rightarrow \infty} F(W_g/\lambda_o) \rightarrow \text{Constant}$$

In view of these properties a trial form for $F(W_g/\lambda_o)$ was assumed to be

$$F(W_g/\lambda_o) = \alpha \tanh \beta W_g/\lambda_o$$

with $\alpha, \beta = \text{constants}$. With this assumption the equation for the attenuation becomes

$$\gamma = \alpha \tanh(\beta W_g/\lambda_o) [C_B/C_o - 1]$$

where

$$C_B/C_o = f(U_g/C_o, d_g/\lambda_o) .$$

The experimental results for γ together with the calculated values of C_B/C_o were used in a least squares analysis to determine α and β . This procedure yielded $\alpha = 4.7$ and $\beta = 1.65$. Figure 21 is a plot of $\gamma/\tanh(1.65 W_g/\lambda_o)$ against $[C_B/C_o - 1]$ for all experimental results for which C_B/C_o was in the range in which γ was linearly increasing with C_B/C_o . The collapse of the experimental data about the line given by

$$\gamma = 4.7 \tanh(1.65 W_g/\lambda_o) [C_B/C_o - 1]$$

suggests that this empirically derived equation satisfactorily summarizes the results of the experiments.

V. MINIMUM POWER REQUIREMENTS

The power required to produce an artificially generated surface current by towing a grid through the water is given by

$$P = \frac{1}{2} \rho C_D (U_g/C_o)^3 (W_g/\lambda_o) (d_g/\lambda_o) C_o^3 \lambda_o^2 ,$$

where the drag coefficient, C_D could vary with the details of the grid construction. For the grids used in the present experiments $C_D = 0.65$. The determination of the choice of parameters, U_g/C_o , d_g/λ_o and W_g/λ_o which will minimize the power required to achieve a given wave attenuation, γ_o , is, in principle, a straightforward optimization problem. The formal mathematical statement of the general problem is:

$$U = f(U_g)$$

$$d = g(d_g)$$

$$W = h(W_g)$$

$$\gamma = \gamma(U/C_o, d/\lambda_o, W/\lambda_o)$$

$$P' = \frac{P}{\frac{1}{2} \rho C_D C_o^3 \lambda_o^2} = (U_g/C_o)^3 (d_g/\lambda_o) (W_g/\lambda_o)$$

find

$$U_g/C_o, \quad d_g/\lambda_o, \quad W_g/\lambda_o$$

such that

$$\gamma = \gamma_o$$

and

$$P' = \text{minimum.}$$

For the present experimental conditions, we have found

$$U = 0.5 U_g$$

$$d = d_g$$

$$W = W_g$$

$$\gamma = 4.7 \tanh(1.65 W_g/\lambda_o) [C_B/C_o - 1]$$

where

$$C_B/C_o = C_B/C_o(U/C_o, d/\lambda_o)$$

is an implicit solution of Equation (21). The complexity of the expression for C_B/C_o prevents us from obtaining an analytic solution to the optimization problem. It was found possible, however, to obtain a solution by essentially a trial and error approach.

To begin, we define a powering coefficient, C_p , as

$$C_p = \frac{P}{\frac{1}{2} \rho C_D C_o^3 \lambda_o^2 W_g/\lambda_o} = (U_g/C_o)^3 (d_g/\lambda_o) .$$

The first step is to determine the combinations of U_g/C_o and d_g/λ_o which provide a minimum value of C_p for a specified value of C_B/C_o . In Figure 22 curves for $C_B/C_o - 1 = \text{constant}$ and $C_p = \text{constant}$ are plotted on a graph of U_g/C_o versus d_g/λ_o . The minimum value of $C_p = (C_p)_{\min}$ was determined by trial and error for several presumed values of the wave celerity ratio C_B/C_o . The results of this procedure are also plotted in Figure 22 and from this plot the combination of values from U_g/C_o and d_g/λ_o which provide the minimum powering coefficient for a given value of $(C_B/C_o - 1)$ can be obtained. In Figure 23 the results of the trial and error procedure are recast with $(C_p)_{\min}$ plotted against $(C_B/C_o - 1)$.

The next step in the determination of the minimum power required to achieve a given attenuation γ_o was to determine the optimum value for W_g/λ_o . The required power is proportional to $C_p W_g/\lambda_o$. The procedure employed to find the minimum value of $C_p W_g/\lambda_o$ can be summarized as follows:

- (1) Select a trial value for W_g/λ_o
- (2) With W_g/λ_o and γ_o specified, the empirically determined equation for γ was used to find the required value of $(C_B/C_o - 1)$ to achieve this attenuation, i.e.,

$$C_B/C_o - 1 = \frac{\gamma_o}{4.7 \tanh(1.65 W_g/\lambda_o)}$$

- (3) From Figure 23 the value of $(C_p)_{\min}$ for the value of $(C_B/C_o - 1)$ found in Step 2 was determined and the product $(C_p)_{\min} W_g/\lambda_o$ was calculated.

- (4) Steps (1) through (3) were repeated for a systematic variation in W_g/λ_o such that the value of W_g/λ_o which provided a minimum value of $(C_p)_{\min} W_g/\lambda_o$ could be determined.

The results of this procedure revealed that the optimum value of W_g/λ_o was 0.85 for γ_o ranging from 50 to 80 percent. With this result the minimum power for a specified attenuation of a given initial wave train may be readily determined.

The minimum required power may be written as

$$P = \frac{1}{2} \rho C_D (C_p)_{\min} (W_g/\lambda_o)^3 C_o^3 \lambda_o^2,$$

and, since the optimum value of $W_g/\lambda_o = 0.85$ and

$$C_o = \frac{gT_o}{2\pi},$$

$$\lambda_o = \frac{gT_o^2}{2\pi}$$

where T_o = the wave period, then

$$P = \frac{1}{2} \rho C_D (C_p)_{\min} (0.85) \left(\frac{g}{2\pi}\right)^5 T_o^7 \quad (22)$$

and for $C_D = 0.65$ and nominal values for ρ and g then

$$P = 3.54 (C_p)_{\min} T_o^7.$$

with P expressed in horsepower and T_0 in seconds. For a specified attenuation γ_0 , the empirical equation for γ is used to determine the required value of $(C_B/C_0 - 1)$. The plot of $(C_p)_{\min}$ against $(C_B/C_0 - 1)$ in Figure 23 is then used to find the appropriate value of $(C_p)_{\min}$.

The results of this procedure are summarized in Table I.

Table I

$\gamma_0(\%)$	$C_B/C_0 - 1$	$(C_p)_{\min}$
50	.12	$.51 \times 10^{-3}$
60	.144	$.90 \times 10^{-3}$
70	.168	1.49×10^{-3}
80	.192	2.30×10^{-3}

The values of $(C_p)_{\min}$ found in Table I may then be used in Equation (22) to obtain the minimum power required to attain the specified attenuation, γ_0 . The results are presented in Table II.

Table II

Wave Characteristics			Minimum Power for Specified Wave Attenuation (horsepower)			
T_0	λ_0	C_0	$\gamma_0 = 50\%$	$\gamma_0 = 60\%$	$\gamma_0 = 70\%$	$\gamma_0 = 80\%$
(sec)	(feet)	(ft/sec)				
2	20.48	10.24	0.2	0.4	0.7	1.0
3	46.08	15.36	3.9	6.9	11.3	17.5
4	81.92	20.48	29.1	51.3	85.0	131.0
5	128.00	25.60	138.7	244.7	405.1	625.3
6	184.32	30.72	496.8	876.8	1452.0	2241.0
7	250.88	35.84	1462.0	2579.0	4270.0	6592.0
8	327.68	40.96	3722.0	6568.0	10874.0	16786.0
9	414.72	46.08	8489.0	1498.0	24801.0	38283.0
10	512.00	51.20	17748.0	31320.0	51852.0	80040.0

VI. SUMMARY AND DISCUSSION OF RESULTS

A series of experiments was performed to determine the attenuation of a sinusoidal surface wave train encountering a laterally sheared surface current of finite width and depth produced by towing a grid through the water. Observations of the velocity distribution within the wake of the grid suggested that for a first approximation the velocity along the centerline of the wake could be characterized as uniform from the surface to a depth equal to the grid draft with the centerline speed equal to one half of the grid tow speed. This approximation was applicable to the region of the wake within a distance of about 2-3 grid widths aft of the grid. With this characterization of the wake velocity structure, the results of a two-dimensional analysis of waves on a finite depth variable current, i.e., Equation (21), was employed to obtain an estimate of the ratio of the wave celerity along the centerline of the wake to that in the undisturbed water, C_B/C_O . For a constant ratio of the grid width to the initial wavelength, W_g/λ_O , the experimentally determined values of the wave attenuation, γ , were shown to increase linearly with increasing values of C_B/C_O . For values of C_B/C_O greater than that required to attain an attenuation of about 80%, the attenuation remained essentially constant at this value. By restricting attention to the range of values of C_B/C_O for which the attenuation varied linearly with C_B/C_O an empirical relationship for γ as a function of C_B/C_O and W_g/λ_O was developed, i.e.,

$$\gamma = 4.7 \tanh(1.65 W_g/\lambda_O) [C_B/C_O - 1]$$

where

$$C_B/C_O = C_B/C_O(U/C_O, d/\lambda_O)$$

and

$$U/C_O = 0.5 U_g/C_O, \quad d/\lambda_O = d_g/\lambda_O.$$

The empirically derived equation for γ was then employed to determine the minimum power required to achieve a specified attenuation of an initial wave train. Table II summarizes the results of this procedure while Figure 22, together with the result that the optimum value of W_g/λ_o is 0.85, may be employed to determine the optimal values of U_g/C_o , d_g/λ_o . As a specific example, we can use the results of the calculations of the minimum power to obtain the optimal values of U_g/C_o , d_g/λ_o , W_g/λ_o in order to achieve a 50% reduction in the initial wave height of waves with period $T_o = 7$ sec, and initial wavelength, $\lambda_o = 250$ feet. For a $\gamma_o = 50\%$, Table I shows that the required value of $(C_B/C_o - 1)$ is 0.12 and Table II indicates the minimum power required for $T_o = 7$ sec is 1460 hp. Tables I and II are based on the use of the optimal value of $W_g/\lambda_o = 0.85$. Since $\lambda_o = 250$ feet, the required grid width is 212 feet. For $(C_B/C_o - 1) = 0.12$ the optimal values for U_g/C_o and d_g/λ_o are found from Figure 22 to be

$$U_g/C_o = 0.14$$

$$d_g/\lambda_o = 0.16$$

and since for the present example, $C_o = 35.8$ ft/sec, $\lambda_o = 250$ feet then the grid characteristics are:

$$U_g = 5.0 \text{ ft/sec}$$

$$d_g = 40 \text{ ft}$$

$$W_g = 212 \text{ ft}$$

The following five features of the experimental results should be emphasized:

(1) The power required to achieve a specified attenuation ratio was shown experimentally to be independent of the initial wave height. If the problem were to be recast such that the wave height within the wake was to be less than some specified value, then the required power would vary directly with the initial wave height.

(2) If we define a characteristic length scale for the wave-current interaction to be the width of the grid, then for a variation by a factor of 4 in this length scale the experimental results revealed no measurable scale effect.

(3) Although difficult to measure with precision, the duration of attenuated waves in the wake of the grid appeared to follow a Froude number scaling law. For our test results the duration was found to be of the order of one minute for a characteristic length scale of 8 feet. For prototype length scales 25 to 50 times larger than that in the experiments the duration would be of the order of 5-7 minutes.

(4) The results obtained in the present experiments are limited to regular wave trains initially propagating in the same direction as the velocity in the wake of a towed grid. The effect of the wake on attenuating random waves with varying initial directions of propagation has not been determined.

(5) The minimum power required to achieve a specified attenuation was determined only for the characteristics of the specific grids used in the experiments. In addition this determination did not account for the technical feasibility of deployment of a grid with the optimal dimensions. It could prove practical from a handling point of view to employ smaller grids and accept the penalty of a larger power requirement.

In conclusion, it appears as a result of these experiments and the subsequent analysis that significant local wave attenuation can be attained with artificially generated surface currents requiring reasonable expenditures of power. It is essential to point out that since the required power increases as the seventh power of the wave period that there is a practical upper limit on the applicability of this method.

VII. REFERENCES

1. Savitsky, D., "Interaction Between Gravity Waves and Finite Turbulent Flow Fields," Eighth Symposium on Naval Hydrodynamics, Hydrodynamics in the Ocean Environment, sponsored by ONR, August 1970, Pasadena, California.
2. Phillips, O.M., The Dynamics of the Upper Ocean, Cambridge University Press, 1966.
3. Taylor, G.I., "The Action of a Surface Current Used as a Breakwater," Proc. Roy. Soc. Series A, Vol. 231, 1955.
4. Lau, J.P., "Steady Surface Wave Pattern in a Shear Flow, Ph.D. Thesis, California Institute of Technology, Pasadena, California, 1968.
5. Ursell, F., "Steady Wave Patterns on a Non-Uniform Steady Flow," Jour. Fluid Mech. Vol. 9, 1960.
6. Maruo, H. and Hayasaki, K., "On the Transfiguration of Water Waves Propagating into a Uniform Wake," Trans. Soc. of Naval Architects of Japan, Vol. 132, 1972.

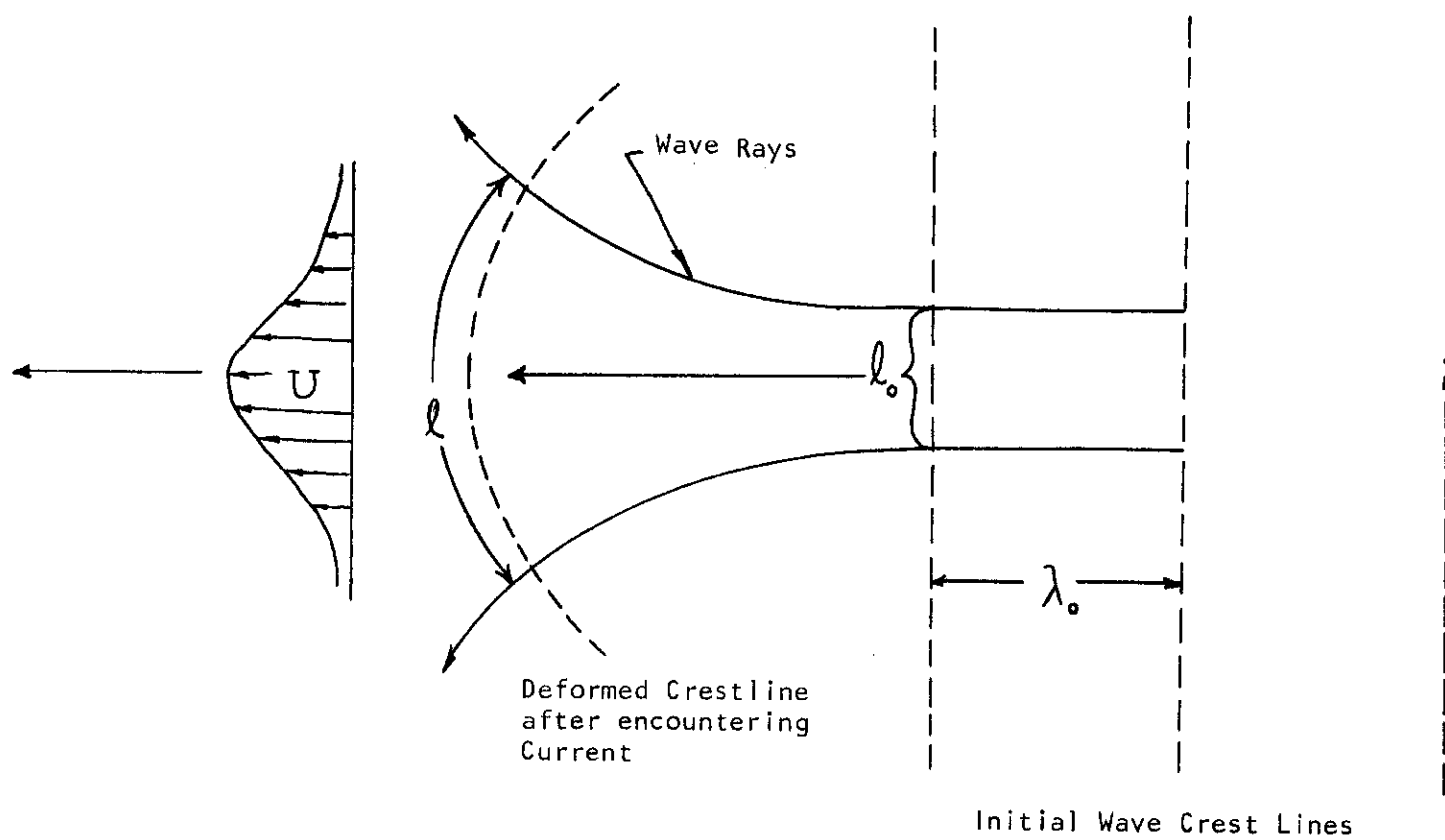


FIGURE 1. Sketch of wave refraction by laterally sheared currents.

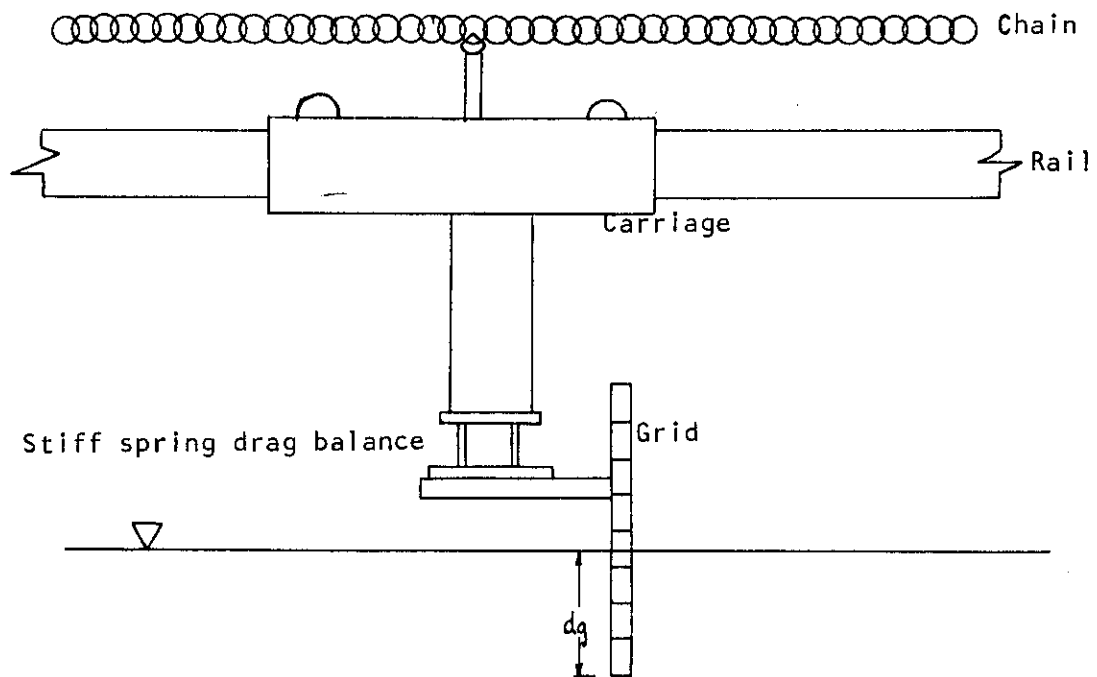


FIGURE 2a. Sketch of the experimental arrangement for towing the grids.

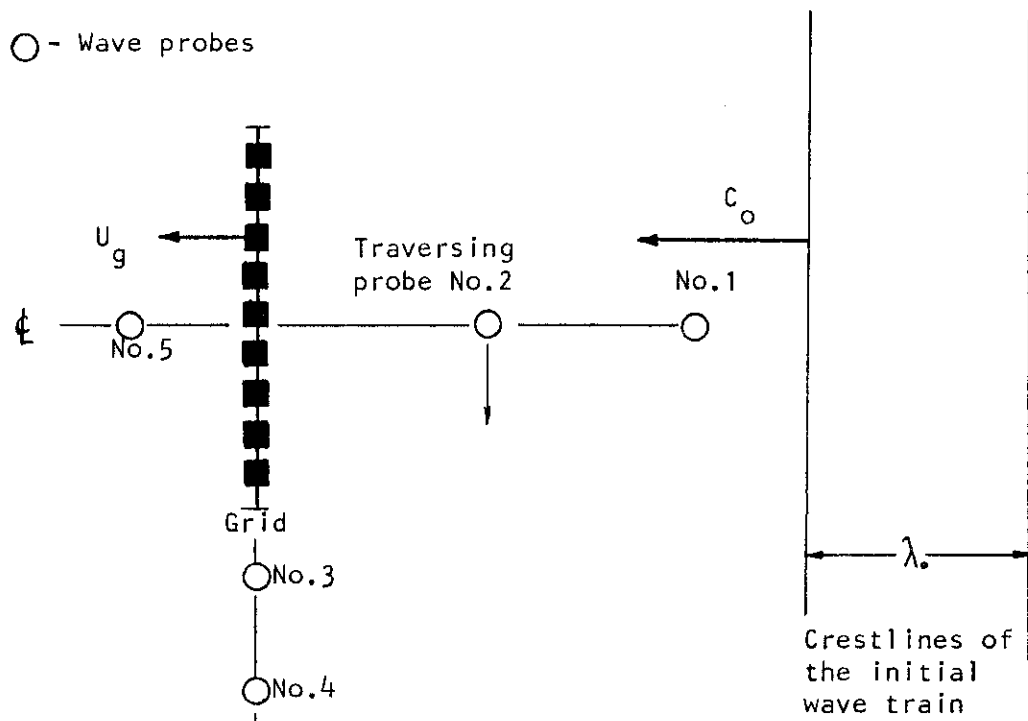
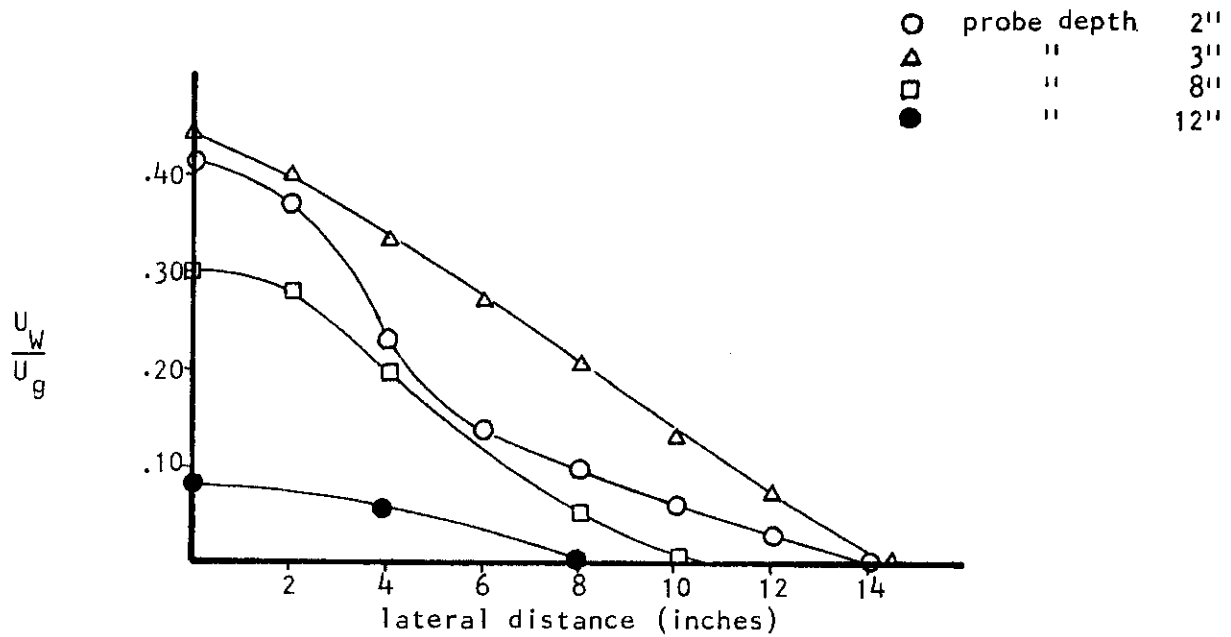
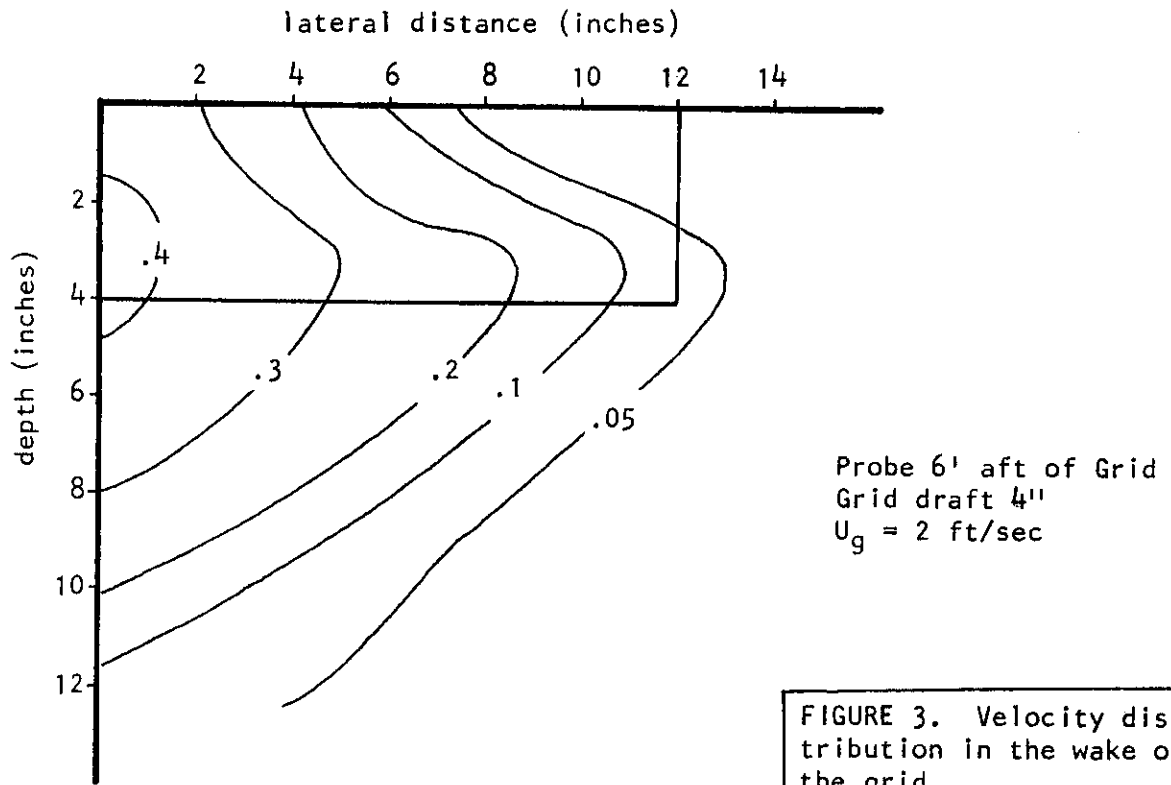
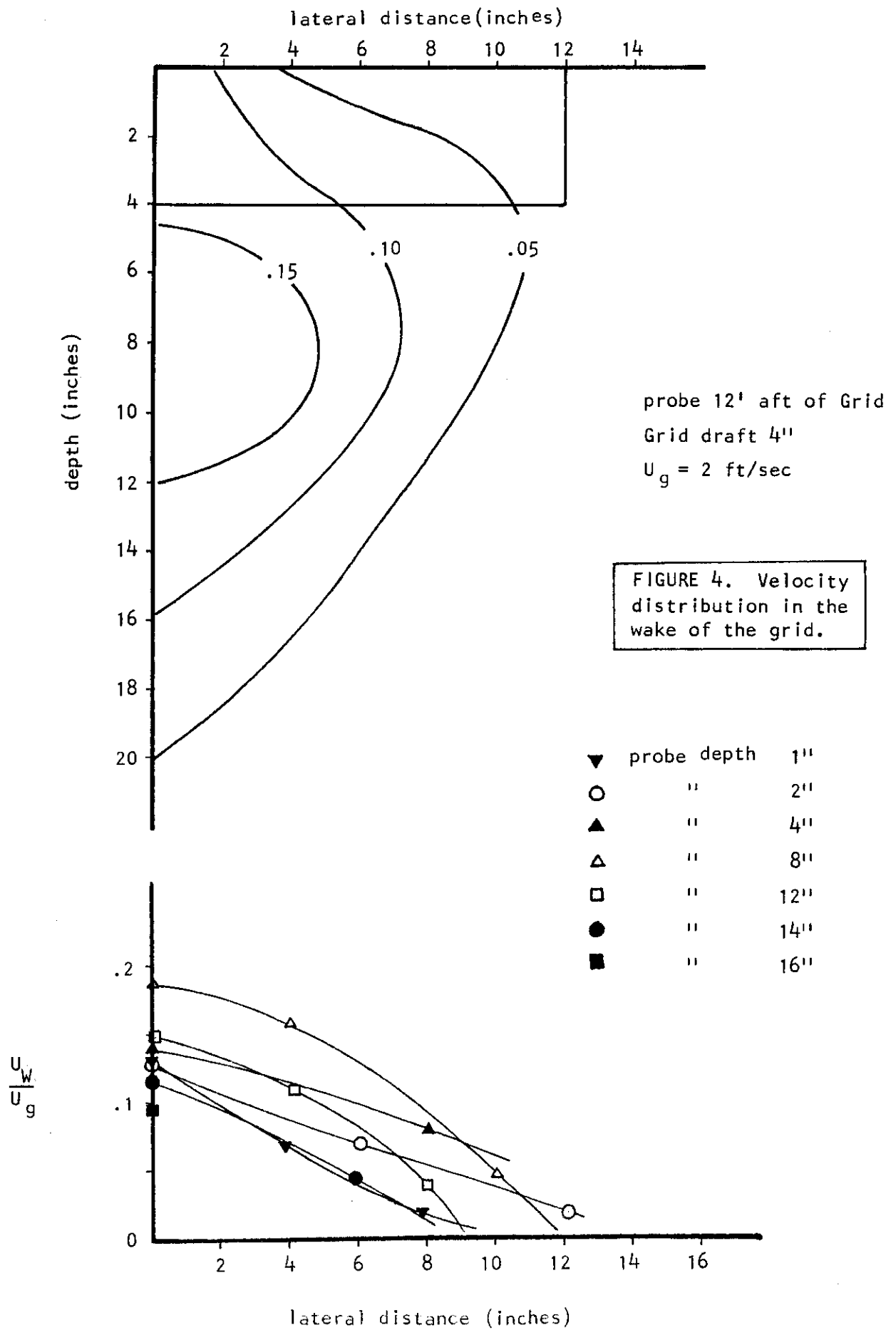
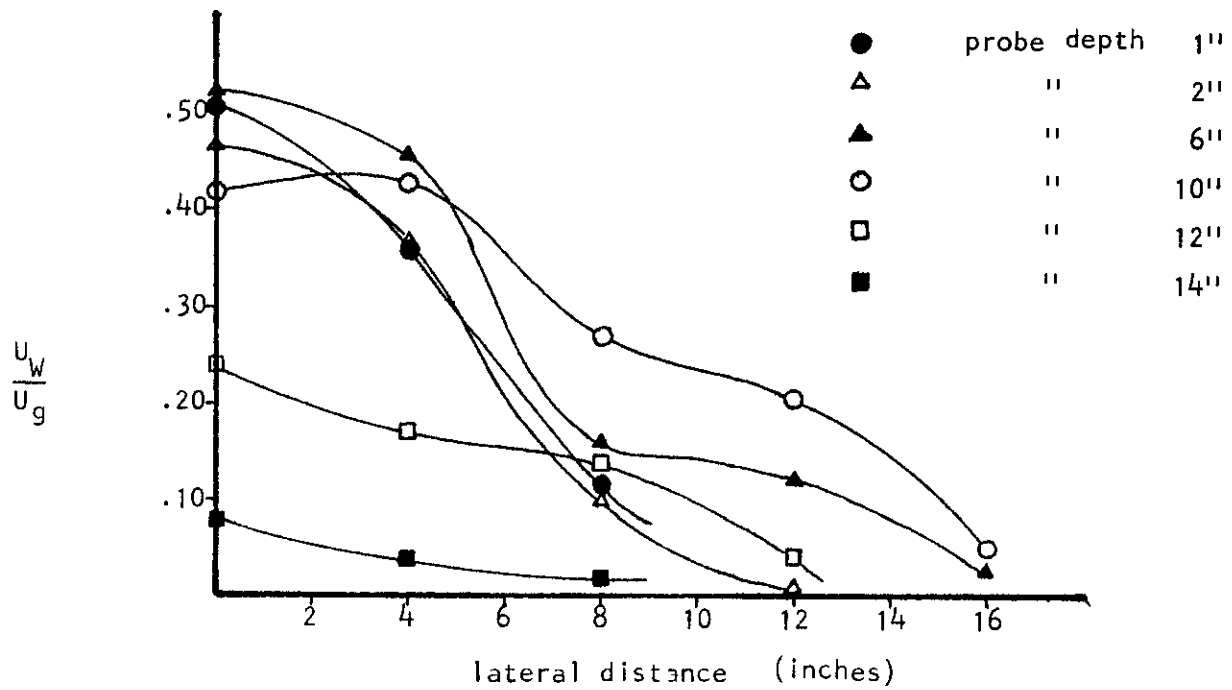
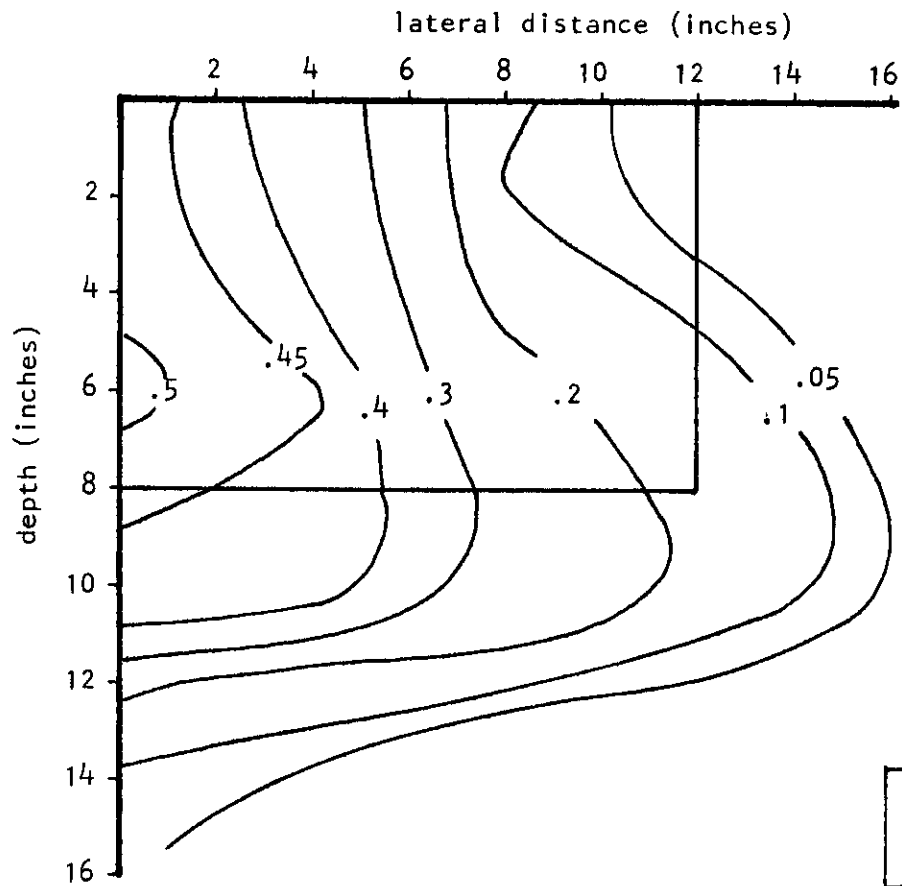
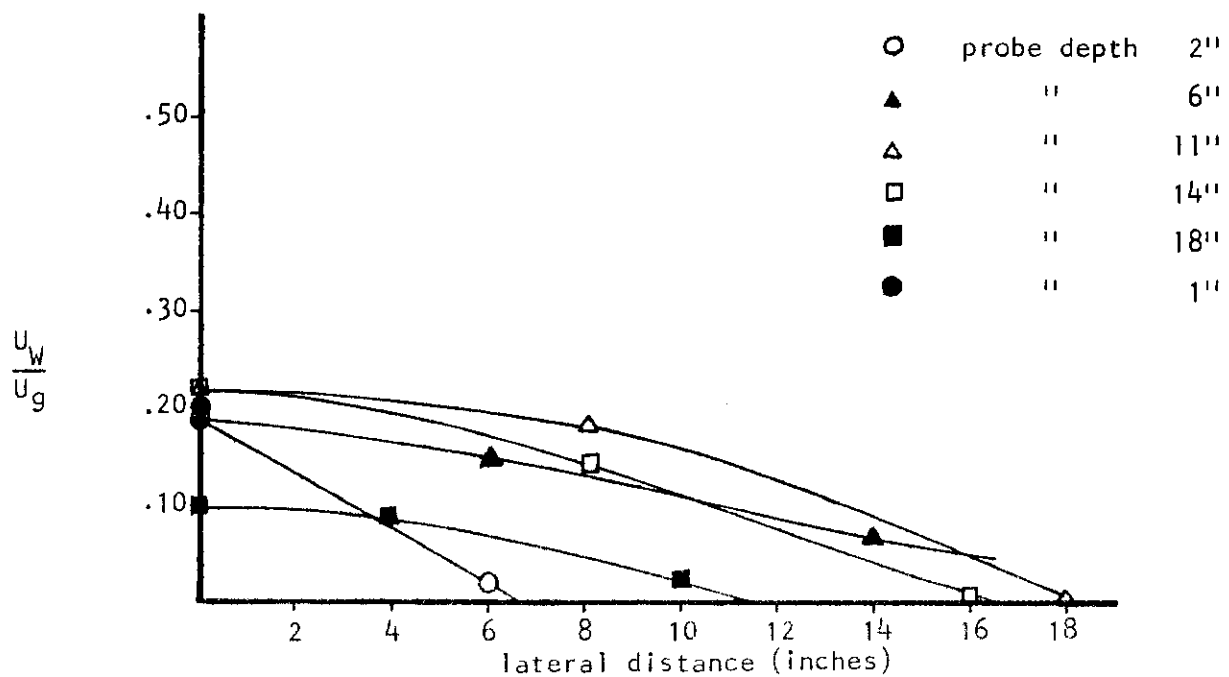
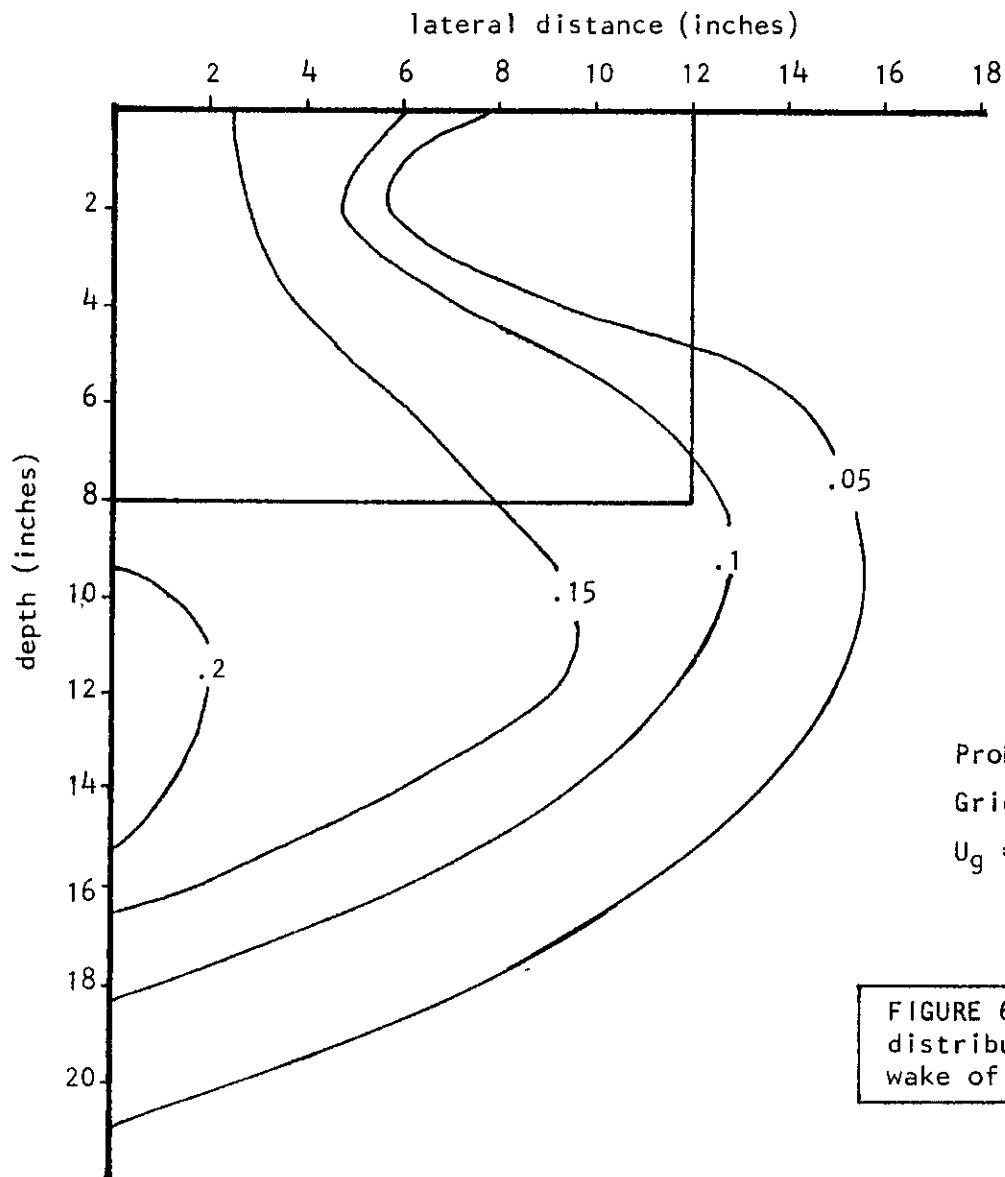


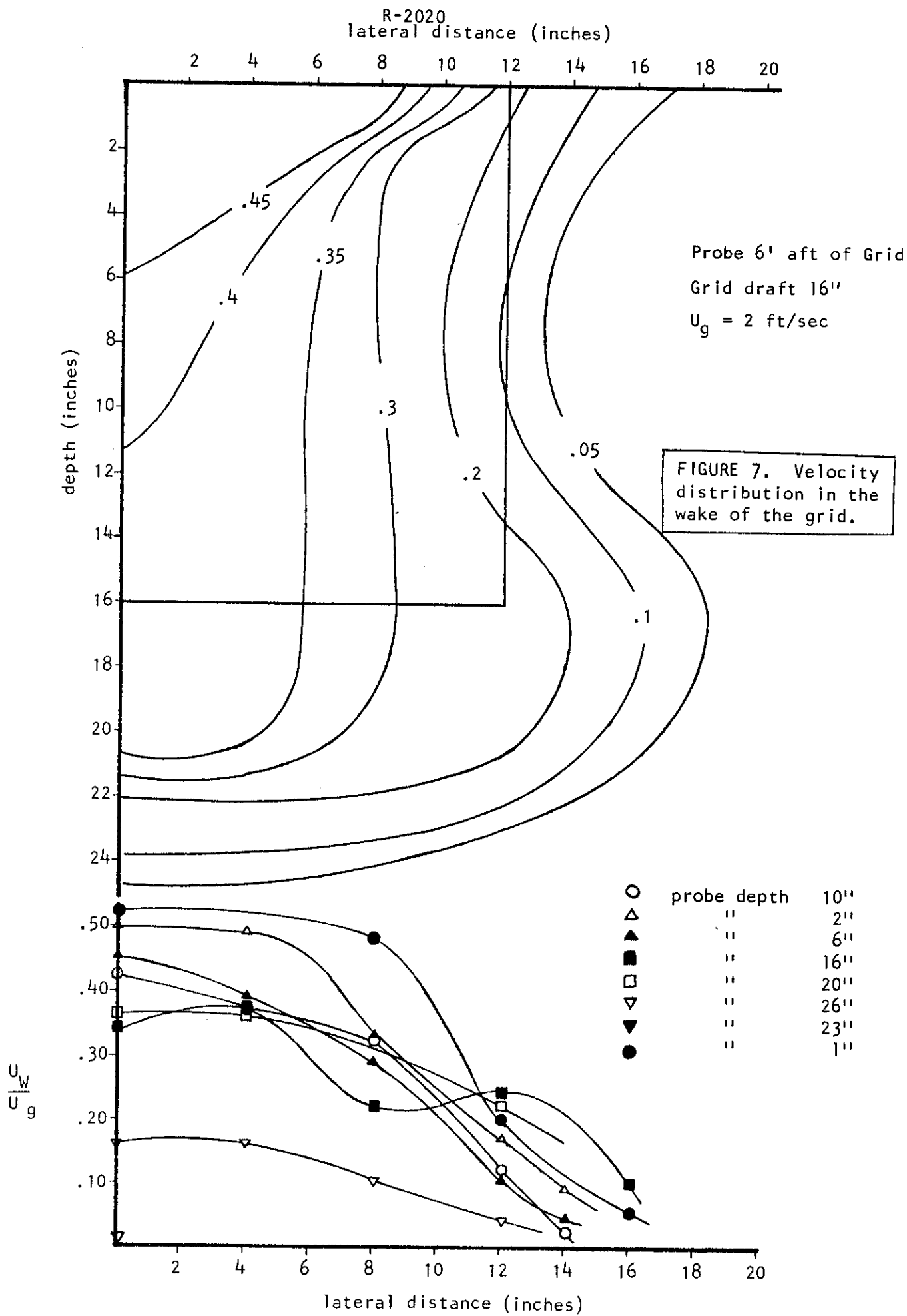
FIGURE 2b. Wave probe arrangement.

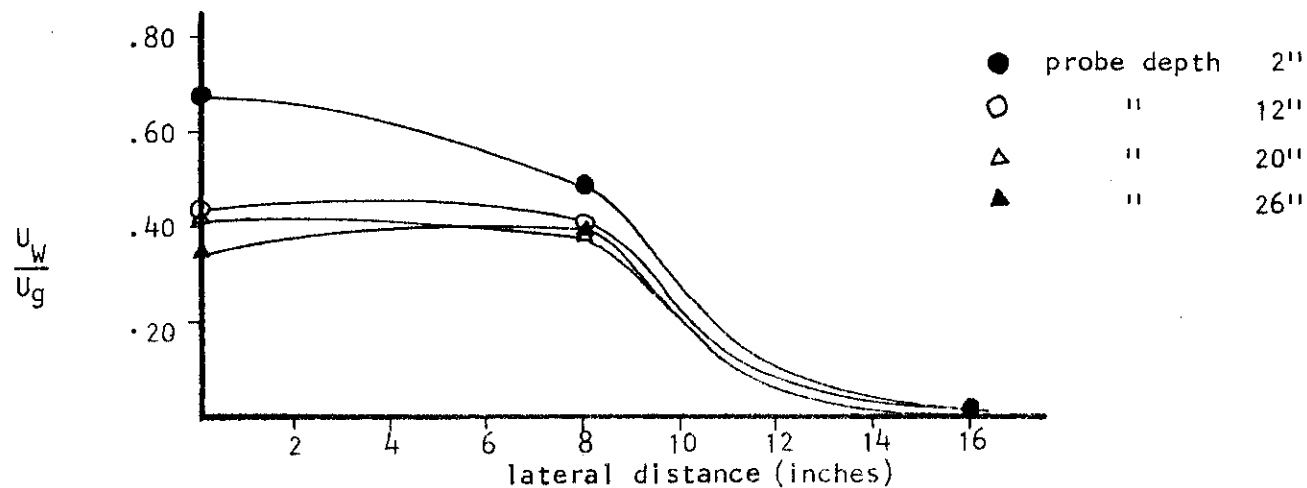
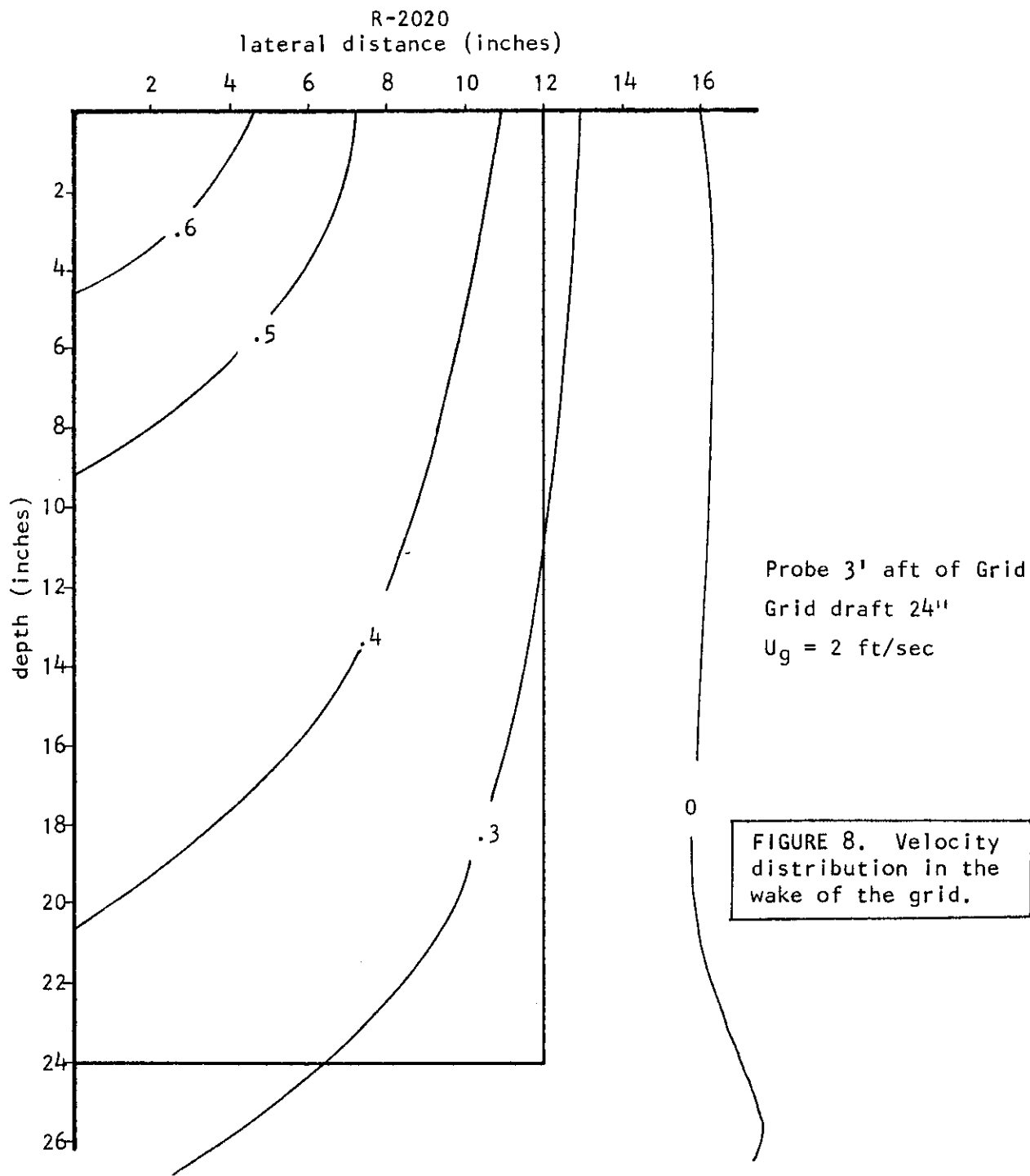


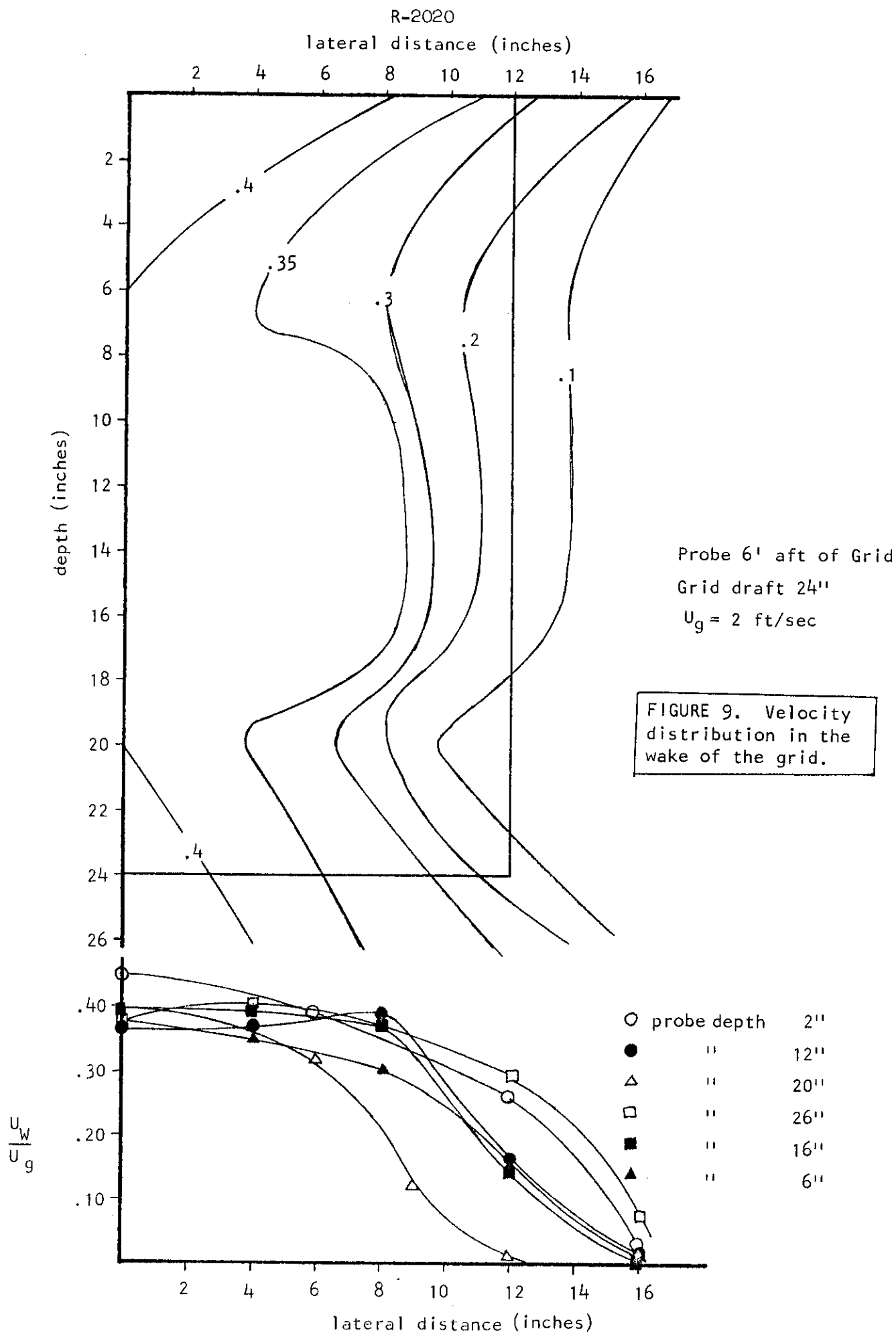


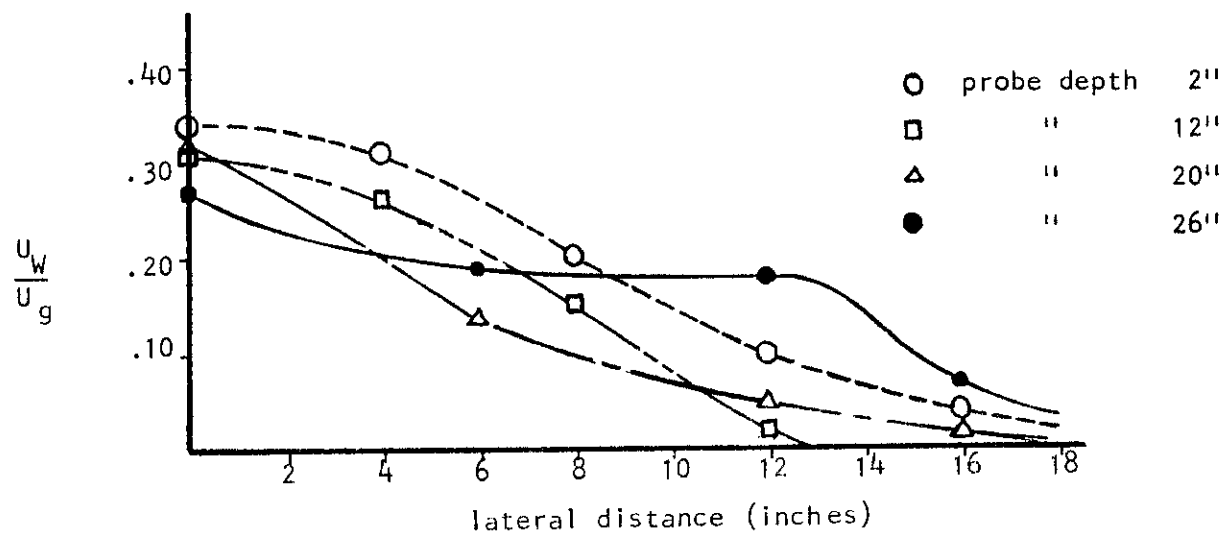
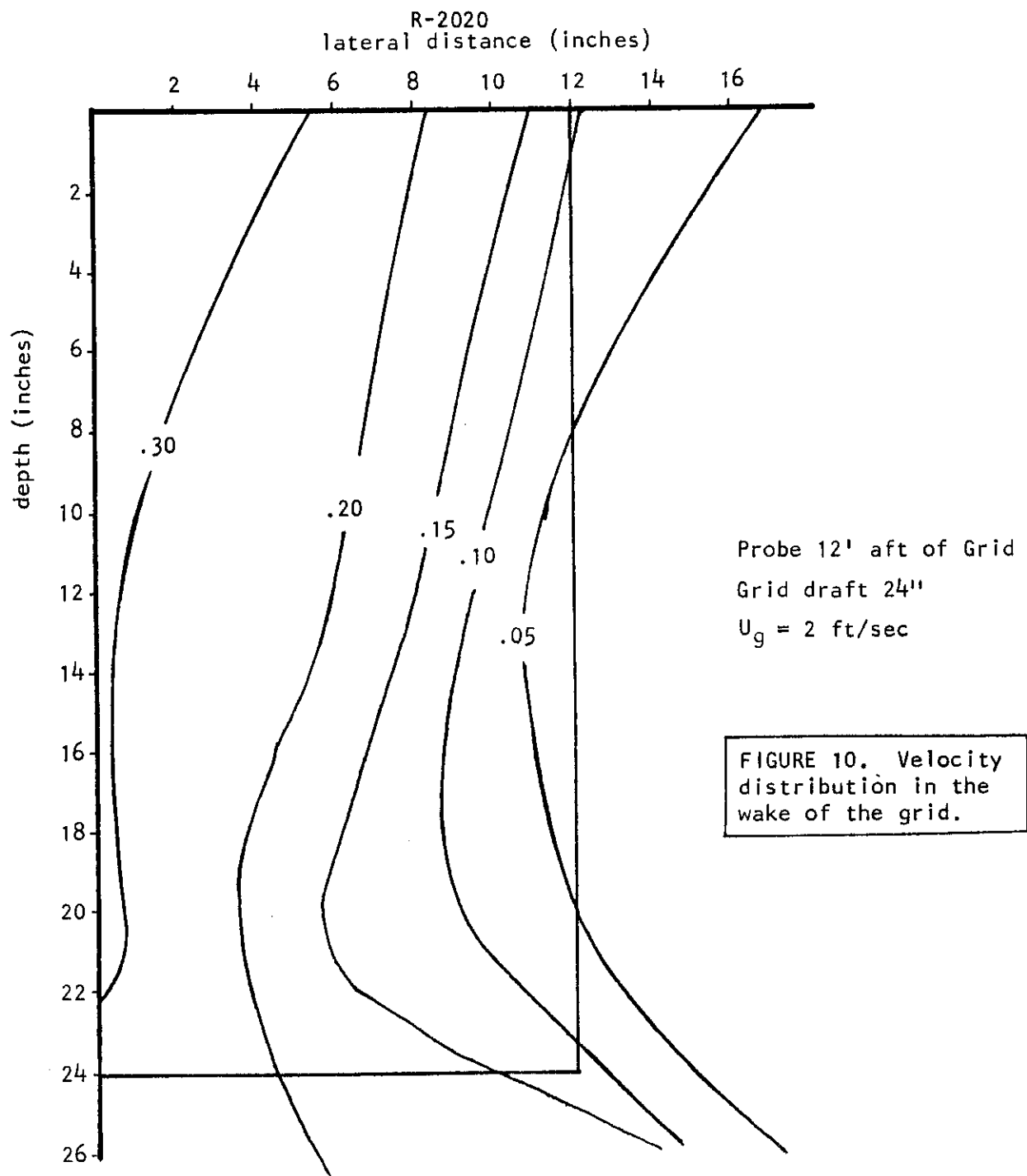


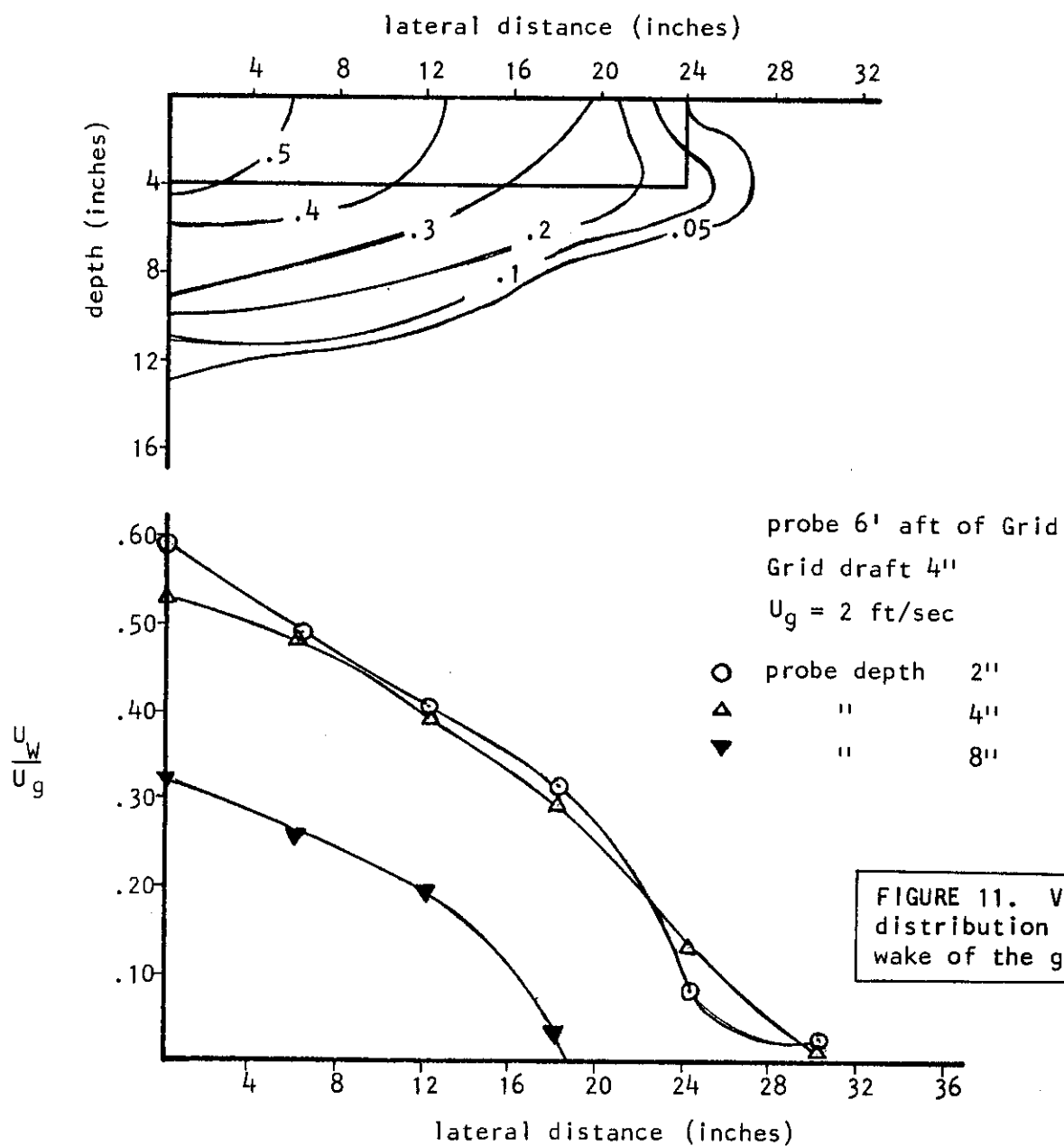












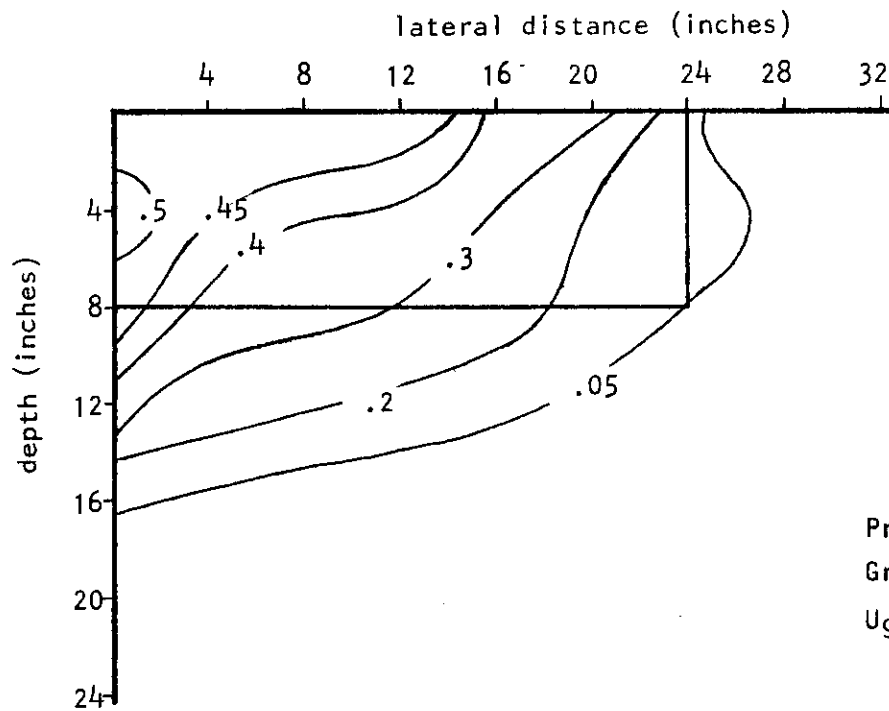
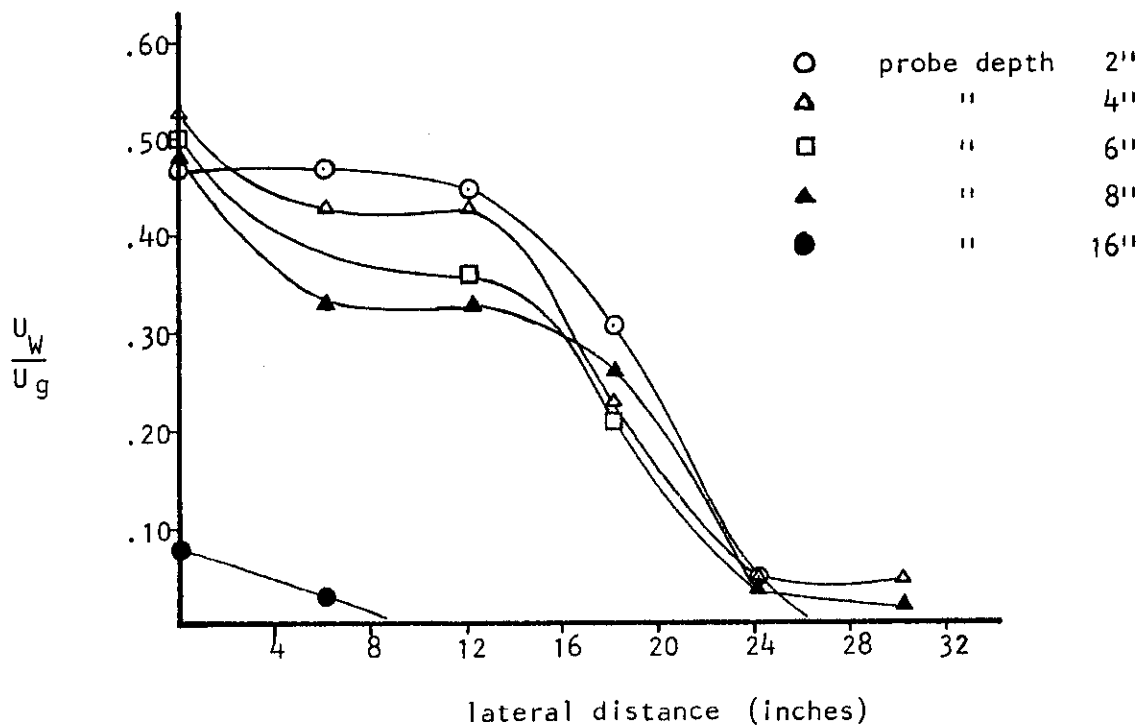


FIGURE 12. Velocity distribution in the wake of the grid.



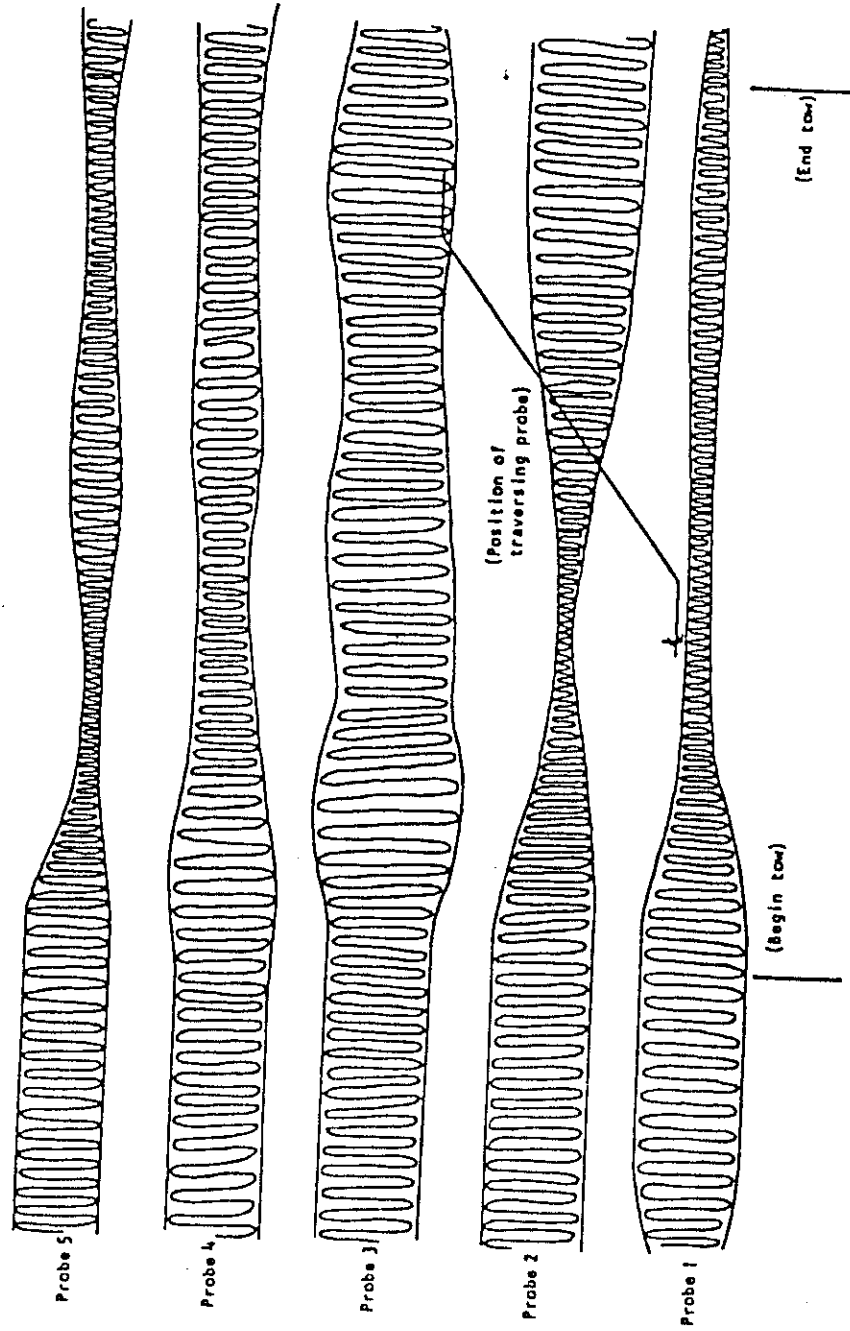
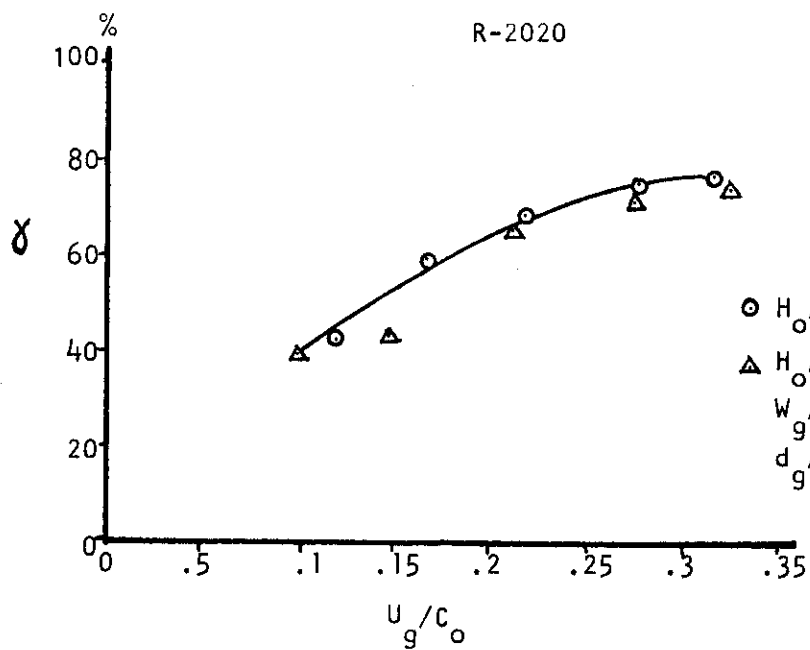
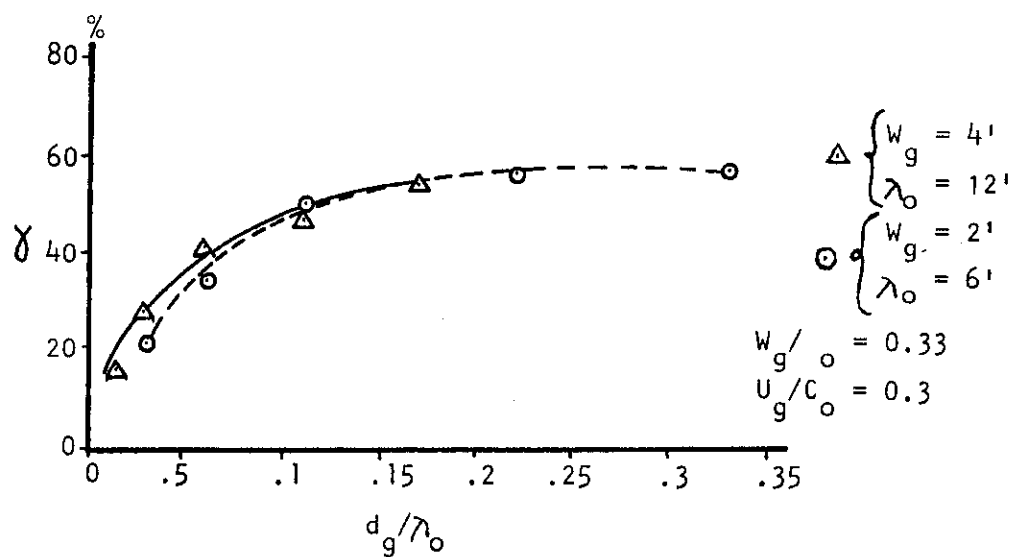


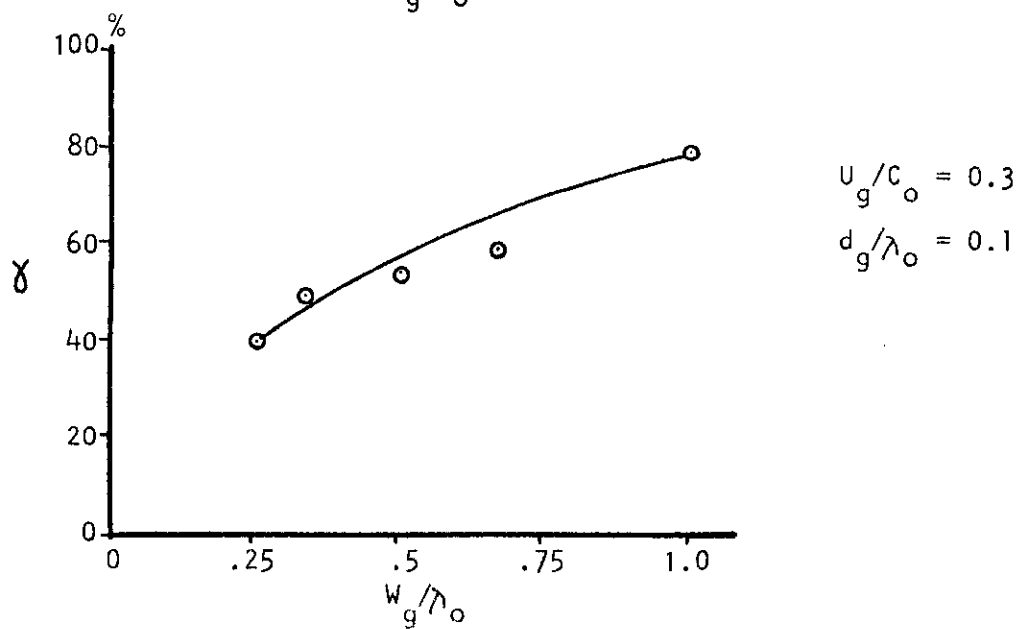
FIGURE 13. Example of wave record for experimental run.



14a.



14b.



14c.

FIGURE 14. Typical variation of wave attenuation with parameters U_g/c_o , d_g/λ_o , and W_g/λ_o .

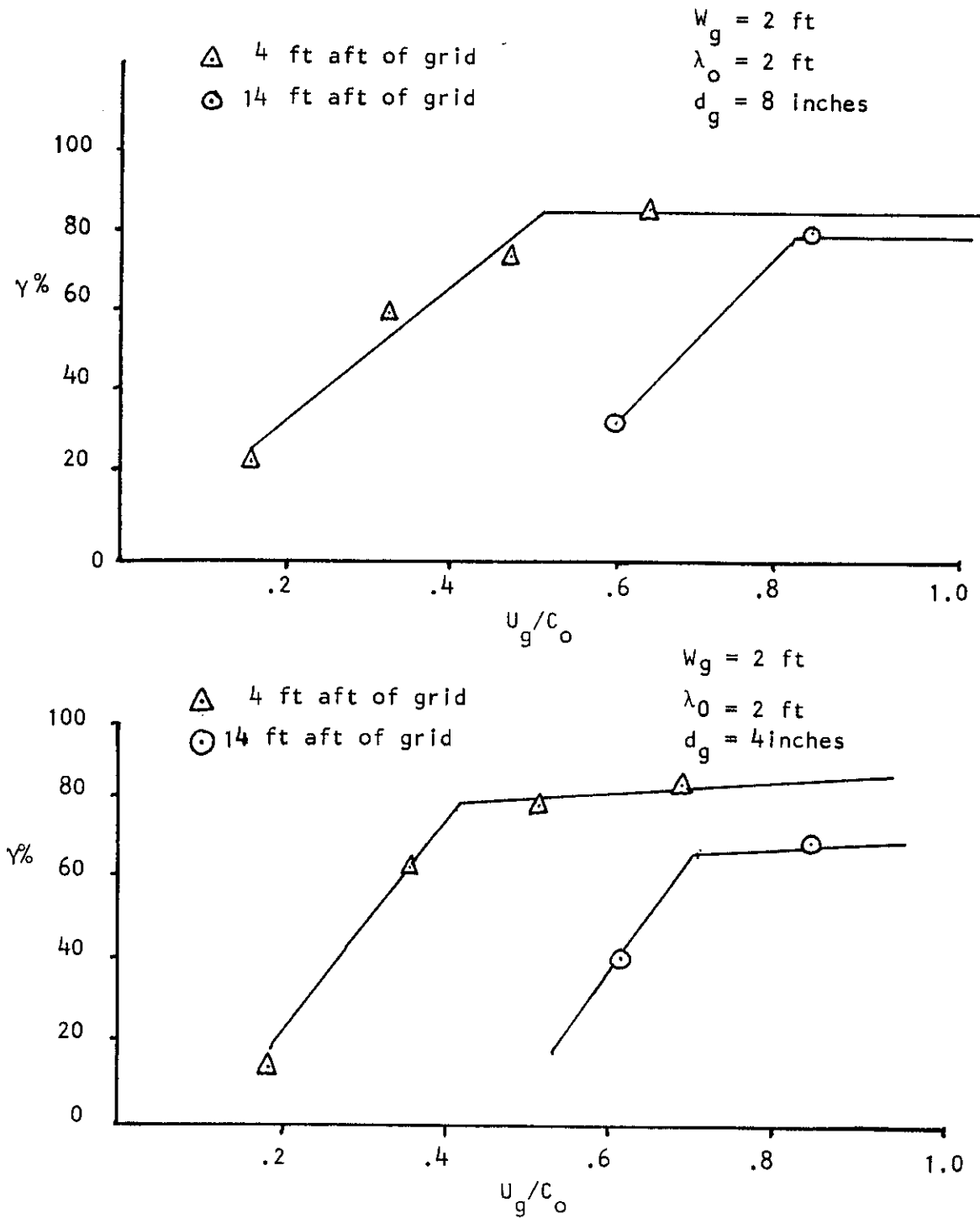


FIGURE 15. Effect of distance aft of grid on wave attenuation.

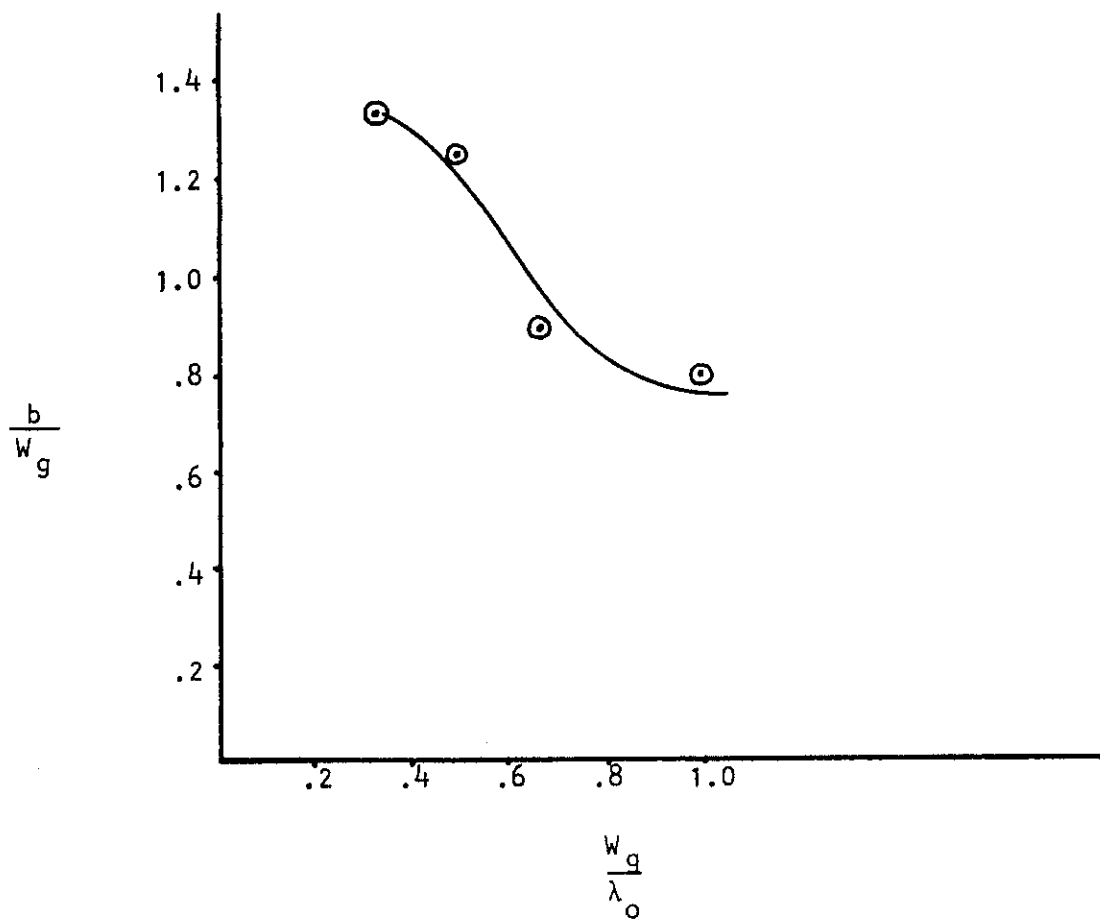


FIGURE 16. Variation of width of the attenuated region with the parameter w_g/λ_o .

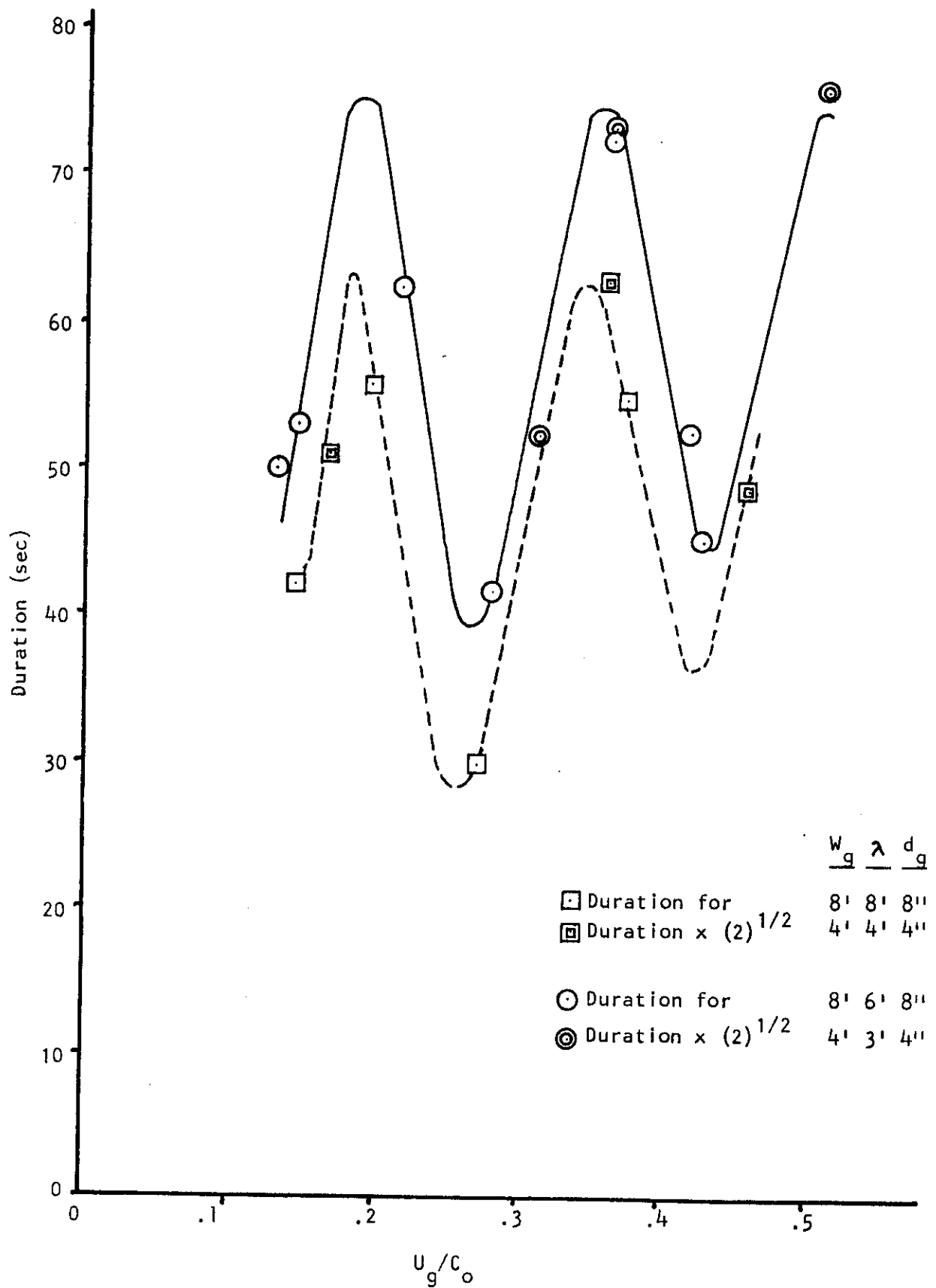
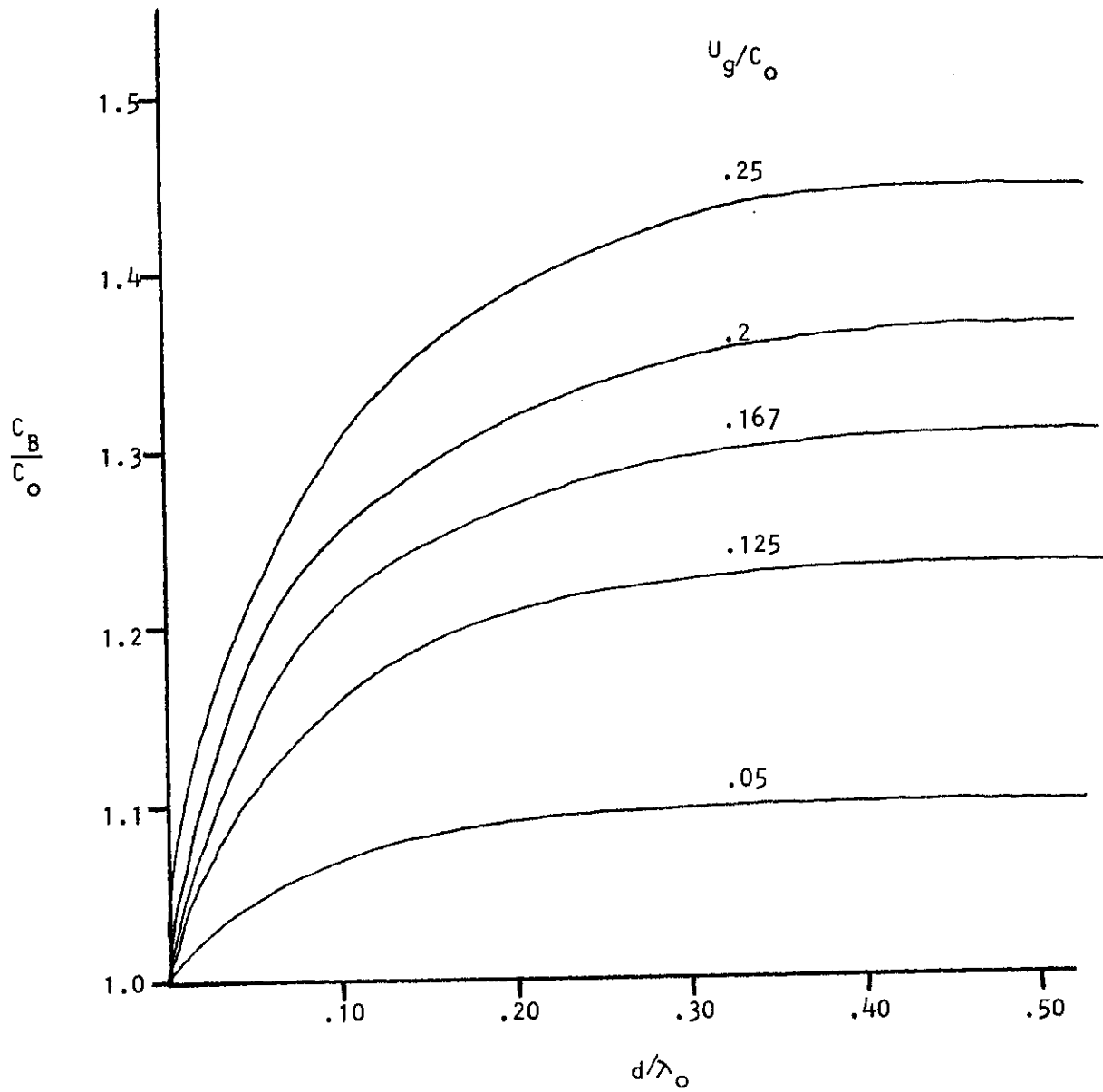


FIGURE 17. Duration of the attenuation following the passage of the grid.

FIGURE 18. Variation of C_B/C_O with d/λ_O .

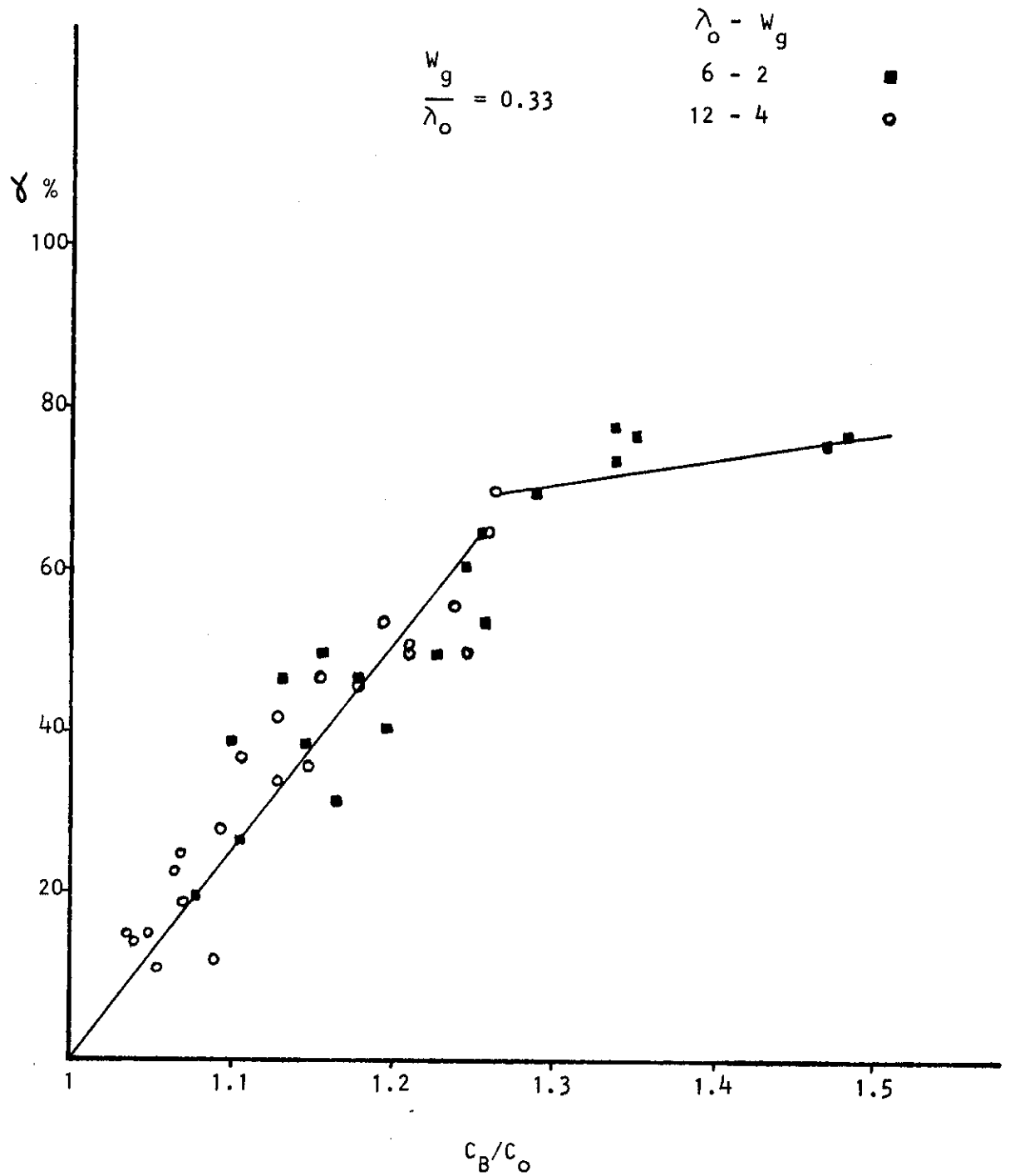
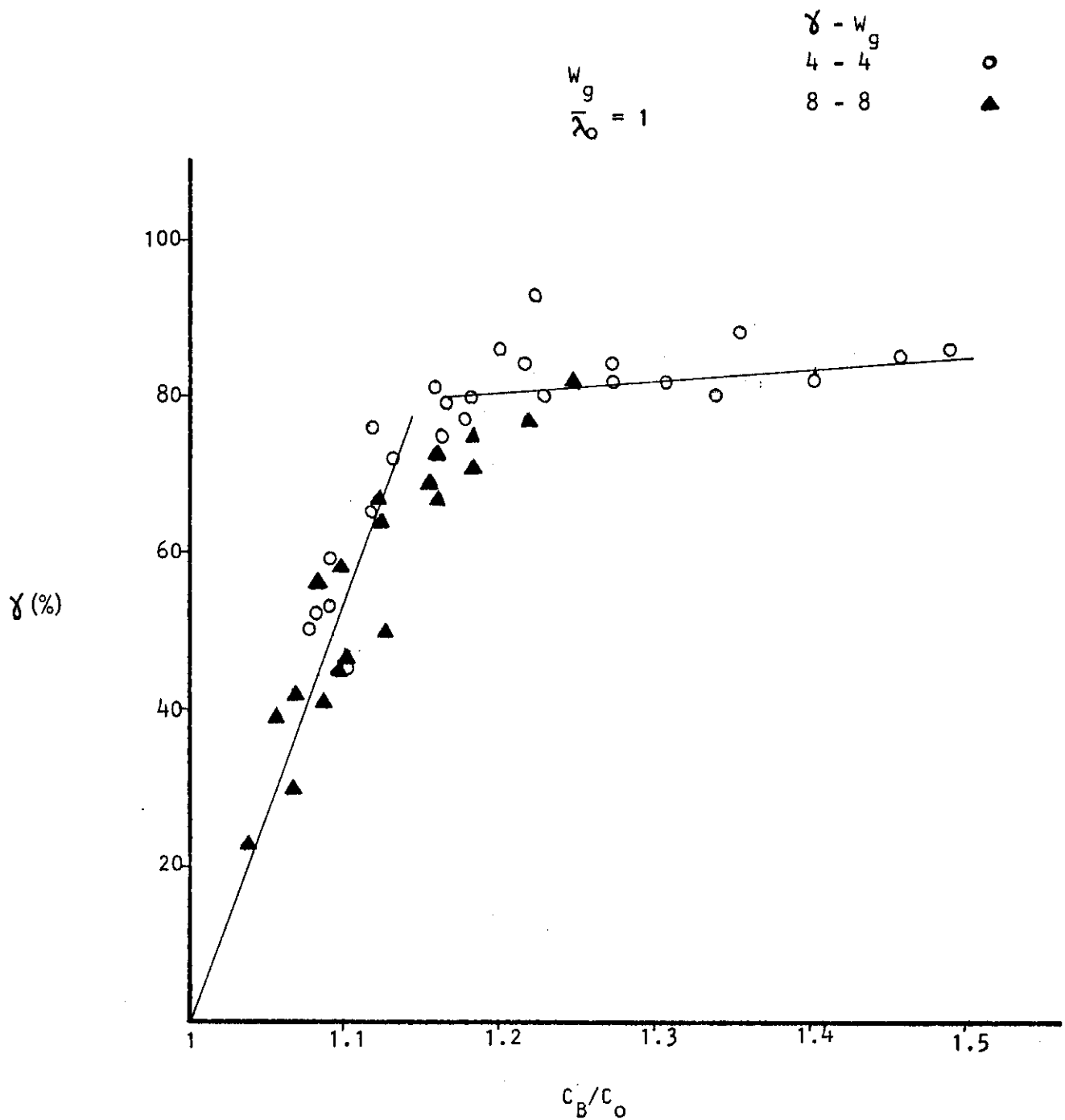


FIGURE 19. Variation of wave attenuation with c_B/c_o .

FIGURE 20. Variation of wave attenuation with c_B/c_0 .

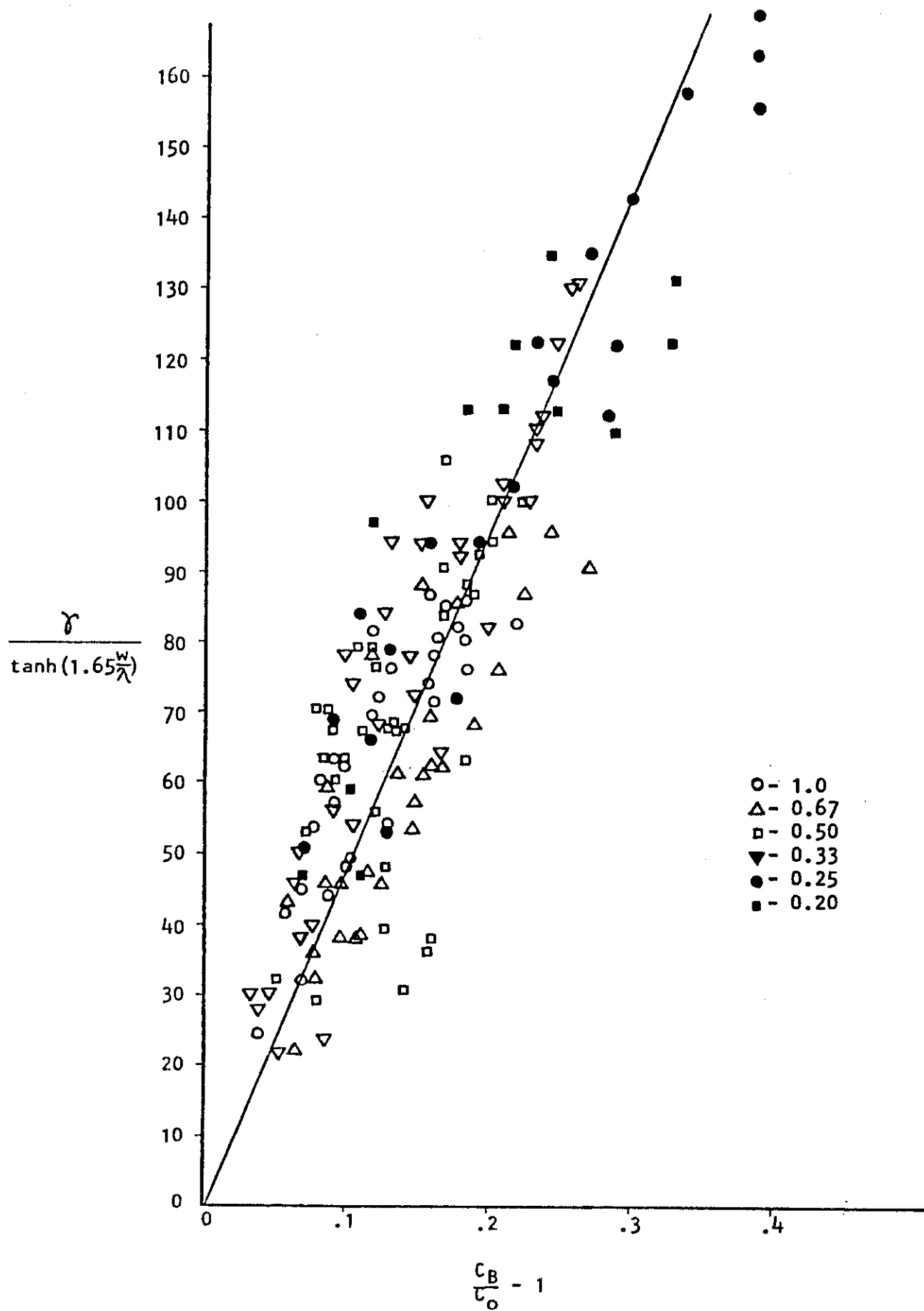


Figure 21. Plot of $\gamma/\tanh(1.65W_g/\lambda_0)$ against calculated values of $c_B/c_0 - 1$

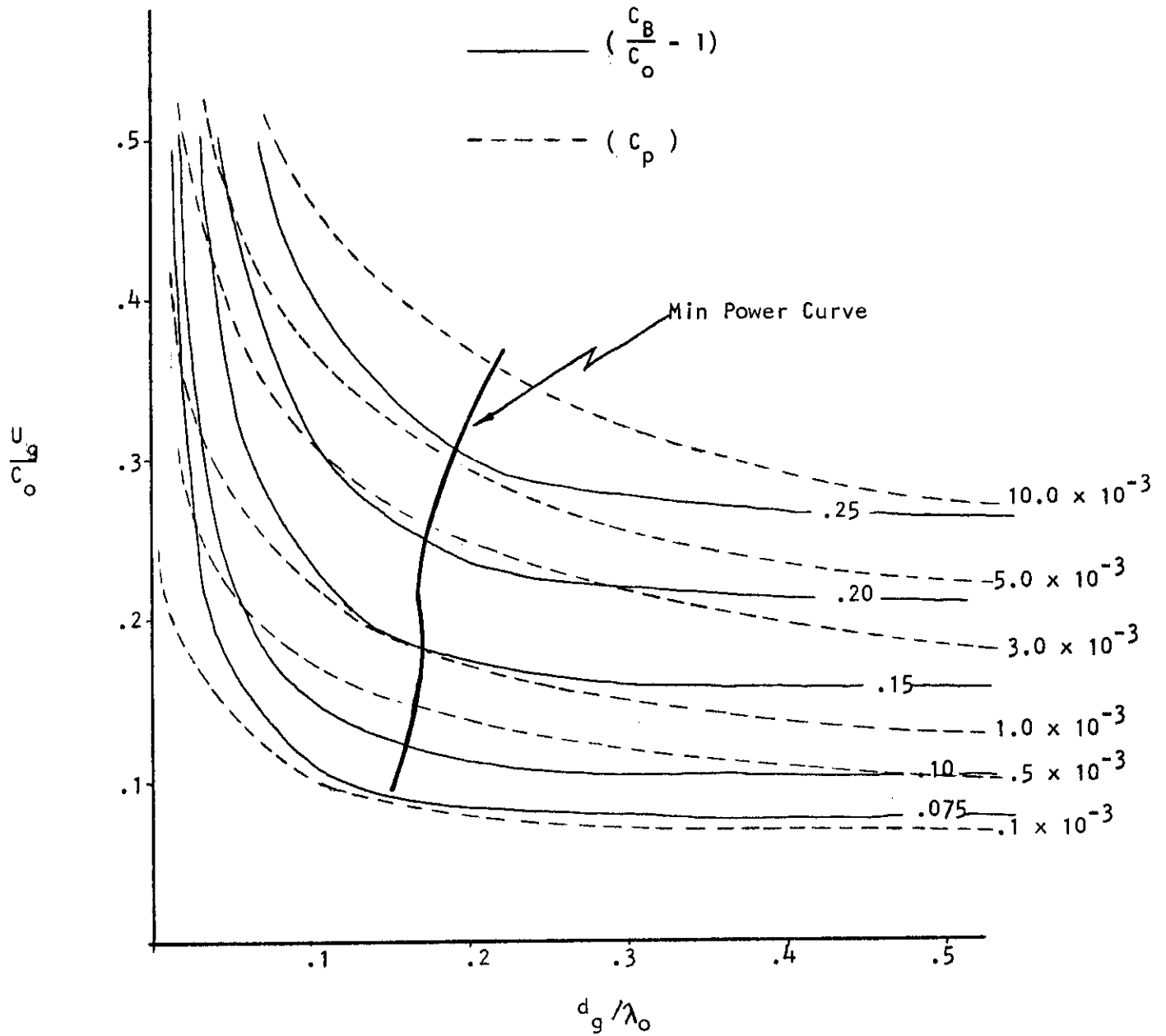


Figure 22. Contours of constant values of $C_B/C_O - 1$ and the powering coefficient C_P on a plot of U_g/C_O versus d_g/λ_O .

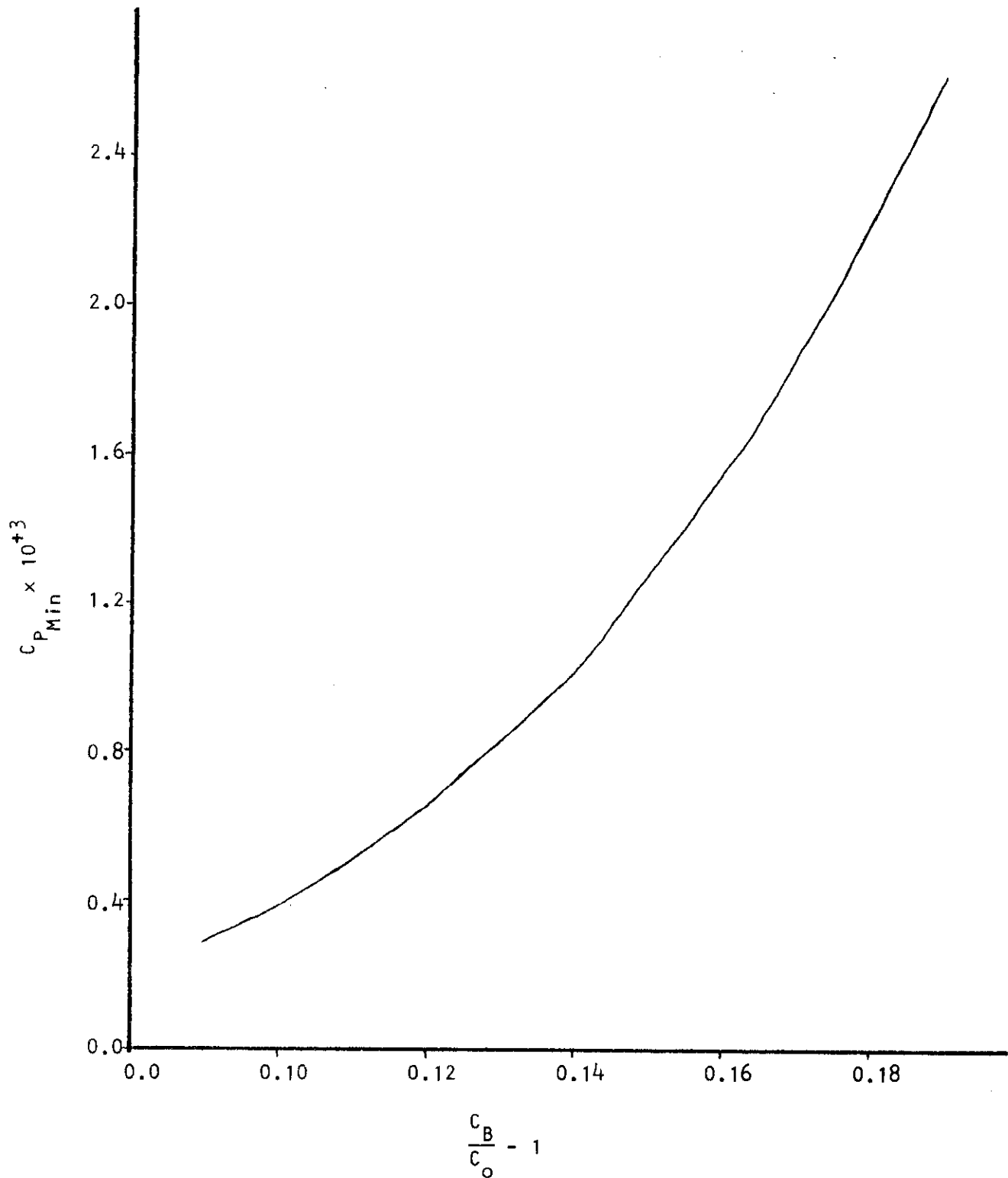


Figure 23. Minimum values of the powering coefficient $(C_p)_{min}$ plotted against $C_B/C_O - 1$.

<p>DAVIDSON LABORATORY, Stevens Institute of Technology Hoboken, New Jersey 07030</p> <p>AN EXPERIMENTAL STUDY OF A METHOD TO ATTENUATE SURFACE WAVES OVER A LIMITED REGION OF THE OPEN OCEAN</p> <p>Report SIT-DL-78-2020 (Final). DL Project 4549/034.</p> <p>Richard I. Hires. June 1978. 28 pages; 23 figures.</p> <p>Contract N00014-77-C-0702 Prepared for Office of Naval Research.</p> <p>Approved for Public Release; Distribution Unlimited.</p>	<p>DAVIDSON LABORATORY, Stevens Institute of Technology Hoboken, New Jersey 07030</p> <p>AN EXPERIMENTAL STUDY OF A METHOD TO ATTENUATE SURFACE WAVES OVER A LIMITED REGION OF THE OPEN OCEAN</p> <p>Report SIT-DL-78-2020 (Final). DL Project 4549/034.</p> <p>Richard I. Hires. June 1978. 28 pages; 23 figures.</p> <p>Contract N00014-77-C-0702 Prepared for Office of Naval Research.</p> <p>Approved for Public Release; Distribution Unlimited.</p>
<p>DAVIDSON LABORATORY, Stevens Institute of Technology Hoboken, New Jersey 07030</p> <p>AN EXPERIMENTAL STUDY OF A METHOD TO ATTENUATE SURFACE WAVES OVER A LIMITED REGION OF THE OPEN OCEAN</p> <p>Report SIT-DL-78-2020 (Final). DL Project 4549/034.</p> <p>Richard I. Hires. June 1978. 28 pages; 23 figures.</p> <p>Contract N00014-77-C-0702 Prepared for Office of Naval Research.</p> <p>Approved for Public Release; Distribution Unlimited.</p>	<p>DAVIDSON LABORATORY, Stevens Institute of Technology Hoboken, New Jersey 07030</p> <p>AN EXPERIMENTAL STUDY OF A METHOD TO ATTENUATE SURFACE WAVES OVER A LIMITED REGION OF THE OPEN OCEAN</p> <p>Report SIT-DL-78-2020 (Final). DL Project 4549/034.</p> <p>Richard I. Hires. June 1978. 28 pages; 23 figures.</p> <p>Contract N00014-77-C-0702 Prepared for Office of Naval Research.</p> <p>Approved for Public Release; Distribution Unlimited.</p>

